Circulation Research
JOURNAL OF THE AMERICAN HEART ASSOCIATION

American Heart Association®
Learn and Live℠

Roles for Endoplasmic Reticulum Associated Degradation and the Novel Endoplasmic Reticulum Stress Response Gene Derlin-3 in the Ischemic Heart

Peter J. Belmont, Wenqiong J. Chen, Matthew N. San Pedro, Donna J. Thuerauf, Nicole Gellings Lowe, Natalie Gude, Brett Hilton, Roland Wolkowicz, Mark A. Sussman and Christopher C. Glembotski

Circ. Res. 2010;106;307-316; originally published online Nov 25, 2009;
DOI: 10.1161/CIRCRESAHA.109.203901
Circulation Research is published by the American Heart Association. 7272 Greenville Avenue, Dallas, TX 72514
 Print ISSN: 0009-7330. Online ISSN: 1524-4571

Roles for Endoplasmic Reticulum–Associated Degradation and the Novel Endoplasmic Reticulum Stress Response Gene Derlin-3 in the Ischemic Heart

Peter J. Belmont, Wenqiong J. Chen, Matthew N. San Pedro, Donna J. Thuerauf, Nicole Gellings Lowe, Natalie Gude, Brett Hilton, Roland Wolkowicz, Mark A. Sussman, Christopher C. Glembotski

Rationale: Stresses, such as ischemia, impair folding of nascent proteins in the rough endoplasmic reticulum (ER), activating the unfolded protein response, which restores efficient ER protein folding, thus leading to protection from stress. In part, the unfolded protein response alleviates ER stress and cell death by increasing the degradation of terminally misfolded ER proteins via ER-associated degradation (ERAD). ERAD is increased by the ER stress modulator, activating transcription factor (ATF)6, which can induce genes that encode components of the ERAD machinery.

Objective: Recently, it was shown that the mouse heart is protected from ischemic damage by ATF6; however, ERAD has not been studied in the cardiac context. A recent microarray study showed that the Derlin-3 (Derl3) gene, which encodes an important component of the ERAD machinery, is robustly induced by ATF6 in the mouse heart.

Methods and Results: In the present study, activated ATF6 induced Derl3 in cultured cardiomyocytes, and in the heart, in vivo. Simulated ischemia (sI), which activates ER stress, induced Derl3 in cultured myocytes, and in an in vivo mouse model of myocardial infarction, Derl3 was also induced. Derl3 overexpression enhanced ERAD and protected cardiomyocytes from simulated ischemia–induced cell death, whereas dominant-negative Derl3 decreased ERAD and increased simulated ischemia–induced cardiomyocyte death.

Conclusions: This study describes a potentially protective role for Derl3 in the heart, and is the first to investigate the functional consequences of enhancing ERAD in the cardiac context. (*Circ Res*. 2010;106:307-316.)

Key Words: endoplasmic reticulum stress ■ unfolded protein response ■ ischemia ■ endoplasmic reticulum-associated degradation

Synthesis and folding of secreted, membrane-bound, and organelle-targeted proteins takes place in the endoplasmic reticulum (ER).[1,2] The ER environment is sensitive to stresses that impair folding of ER proteins.[2] The aggregation of misfolded proteins can be toxic and has been implicated in nearly sixty diseases,[3] including desmin-related cardiomyopathy.[4] In addition, a recent study has shown that transgenic overexpression of preamyloid oligomers is toxic to cardiomyocytes.[5]

An accumulation of misfolded ER proteins triggers the ER stress response (ERSR), also known as the unfolded protein response (UPR),[6] in many different cell and tissue types.[7–9] Initial ERSR signaling is oriented toward resolving the stress and reducing the protein folding load on the ER, leading to survival. Such prosurvival responses include ER-associated protein degradation (ERAD), through which terminally misfolded proteins that accumulate in the ER are degraded. Terminally misfolded ER proteins are translocated out of the ER lumen to be degraded by ERAD.[10] Although the importance of ERAD in the heart has been discussed,[11,12] few studies have analyzed the functionality of ERAD in the myocardium.

Although many details of ERAD remain to be elucidated, it is believed that in part, the activating transcription factor (ATF)6 branch of the ERSR induces some of the ERAD genes. ATF6 is an ER-transmembrane protein that is cleaved on ER stress; the N-terminal fragment of ATF6 translocates to the nucleus and acts as a transcription factor to induce numerous protective ERSR genes. ATF6 can bind to *cis* regulatory elements in ERSR genes, including the ER stress response element (ERSE), ERSE-II, and, to a lesser extent, the unfolded protein response element (UPRE).[13]

To investigate the effects of ATF6 and ERAD in the heart we generated a line of transgenic (TG) mice featuring

Original received June 29, 2009; revision received November 12, 2009; accepted November 16, 2009.

From the San Diego State University Heart Institute and the Department of Biology, San Diego State University, Calif.

Correspondence to Christopher C. Glembotski, The SDSU Heart Institute and the Department of Biology, San Diego State University, San Diego, CA 92182. E-mail cglembotski@sciences.sdsu.edu

Circulation Research **is available at http://circres.ahajournals.org** **DOI: 10.1161/CIRCRESAHA.109.203901**

Non-standard Abbreviations and Acronyms

A1ATmut	α-1 antitrypsin mutant
AdV	adenoviral
ATF	activating transcription factor
CHOP	C/EBP homologous protein
Derl	Derlin
DN	dominant negative
ER	endoplasmic reticulum
ERAD	endoplasmic reticulum–associated degradation
ERSE	endoplasmic reticulum stress–response element
ERSR	endoplasmic reticulum stress response
GRP	glucose-regulated protein
MER	mutant mouse estrogen receptor
miDerl3	microRNA directed to Derl3
miRNA	microRNA
NRVMC	neonatal rat ventricular myocyte cultures
NTG	nontransgenic
PI	propidium iodide
RT-qPCR	quantitative RT-PCR
sI	simulated ischemia
sI/R	simulated ischemia/reperfusion
TG	transgenic
TM	tunicamycin
UPR	unfolded protein response
UPRE	unfolded protein response element

cardiac-restricted expression of a novel protein in which the mutant mouse estrogen receptor (MER) was fused to the C terminus of the active fragment of ATF6. This fusion protein, ATF6-MER, is constitutively expressed in ATF6-MER TG mouse hearts, but is active only on tamoxifen administration.[14] Activation of ATF6 in TG mouse hearts enhances function and reduces necrosis and apoptosis during ex vivo I/R,[14] suggesting that ATF6 contributes to reducing damage and enhancing recovery from I/R. It is possible that some of these effects might be exerted through ATF6-mediated enhancement of ERAD.

Whole-genome microarray analyses of ATF6-MER TG mouse hearts showed that 381 transcripts exhibited ATF6-dependent increases.[15] One of the most induced genes was Derlin-3 (Derl3), a member of a family comprised of Derl1, -2, and -3. The Derlins were named "der" for "degradation in the ER."[16] Derl1 facilitates the retro-translocation of misfolded proteins from the ER lumen to the cytosolic face of the ER.[17] Thus, it is possible that the other Derl family members, including Derl3, exert similar functions.

Although studies of Derl1, -2, and -3 have been done with noncardiac cell types,[18] the mechanism of Derl3 induction in any cell type is unknown, and the Derlin family has not been studied in the heart. Accordingly, we examined the mechanism of induction and function of Derl3 in the heart.

Methods

Animals

The transgenic mice used in this study have been described previously.[14] Approximately 100 neonatal rats and 24 adult male mice were used in this study. All procedures involving animals were in accordance with the San Diego State University Institutional Animal Care and Use Committee.

Cultured Cardiac Myocytes

Primary neonatal rat ventricular myocyte cultures (NRVMCs) were prepared and maintained in culture, as previously described.[19]

An expanded Methods section is available in the Online Data Supplement at http://circres.ahajournals.org.

Results

Promoter Sequence Analysis of ATF6-Regulated Genes in the Heart Identifies Derl3

We previously identified ATF6-regulated genes in ATF6-MER TG mouse hearts.[15] To determine which of the genes from the microarray analyses of ATF6-MER TG mouse hearts might be direct targets of ATF6, the regulatory regions of each were analyzed for the ATF6 binding sites, ERSE, ERSE-II and UPRE.[20–22] ERSE, ERSE-II and UPRE sequences were found 9.6-, 8.4- and 2.1-fold more frequently, respectively, than in the whole mouse genome (Figure 1). Among the 607 ATF6-regulated genes in the heart, 16 have canonical ERSEs, ERSE-IIs, and/or UPREs (Online Tables I through III), whereas 211 have elements, with 1 mismatch (Online Tables IV through VI); mismatches of 1 bp have been shown in other studies to be potential ATF6-binding elements.[13,20] Thus, 227 genes are likely to be direct targets of ATF6.

One of only 2 ATF6-regulated genes with 2 canonical ERSEs is Derlin-3 (see Online Table I; Derl3, NM_024440). Because it may play a role in ERAD, we investigated the mechanism of induction and the function of Derl3 in the heart and cultured cardiac myocytes. To examine transcriptional regulation cultured cardiac myocytes were transfected with several luciferase reporter constructs (Figure 2A) with or without subsequent infection with either a control (AdVCon) or an adenovirus that encodes activated ATF6 (AdVATF6). Luciferase activation in cultures infected with AdVATF6 and transfected with reporter construct 1 was 200-fold of control (Figure 2B, bar 4). ATF6-mediated luciferase induction was reduced by 75% to 80% in constructs 2 and 3, which each contain 1 mutated ERSE (Figure 2B, bars 5 and 6). The ERSR activator tunicamycin (TM) conferred robust induction of construct 1 (Figure 2B, bar 7); however, constructs 2 and 3 exhibited decreased induction (Figure 2B, bars 8 and 9). Thus, maximal ATF6- or TM-mediated induction of the Derl3 promoter was dependent on both ERSE1 and ERSE2.

ATF6 Induces Derl3 in Mouse Hearts

The ability of ATF6 to induce the other Derlin family members was also examined. Whereas neither Derl1 nor Derl2 was induced by tamoxifen in the ATF6 TG mouse hearts (Figure 3A, bars 1 through 8), Derl3 was induced by 400-fold by tamoxifen, but only in the TG mouse hearts (Figure 3A, bars 9 through 12); thus, only Derl3 was ATF6-inducible in the heart, consistent with the lack of ERSEs in the Derl1 and Derl2 genes (Online Table I).

Derlin levels were relatively low in sections from vehicle-treated ATF6-MER TG hearts (Figure 3B, Derl3) and tamoxifen-treated nontransgenic (NTG) mouse hearts (not

A ERSE

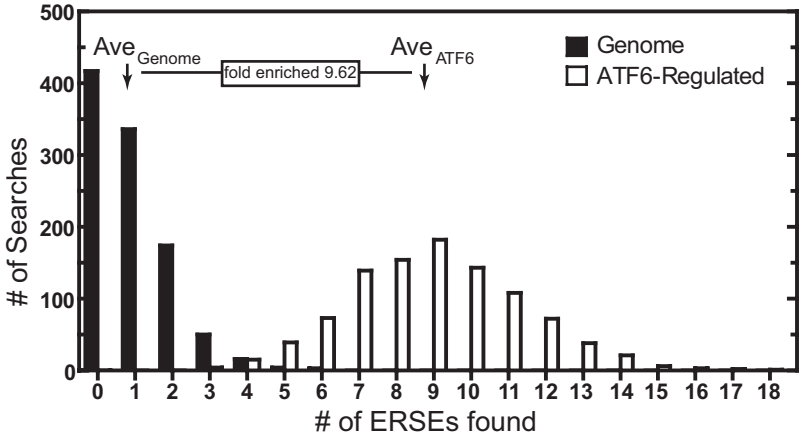

B ERSE Totals

# of ERSEs Found	Genome Searches	ATF6-Regulated Searches
0	417	0
1	336	0
2	174	0
3	50	4
4	16	15
5	4	39
6	3	73
7	0	139
8	0	154
9	0	182
10	0	143
11	0	108
12	0	72
13	0	38
14	0	21
15	0	6
16	0	3
17	0	2
18	0	1
Ave # of ERSEs found:	0.94	9.01

Fold Enrichment: 9.62

C ERSEII

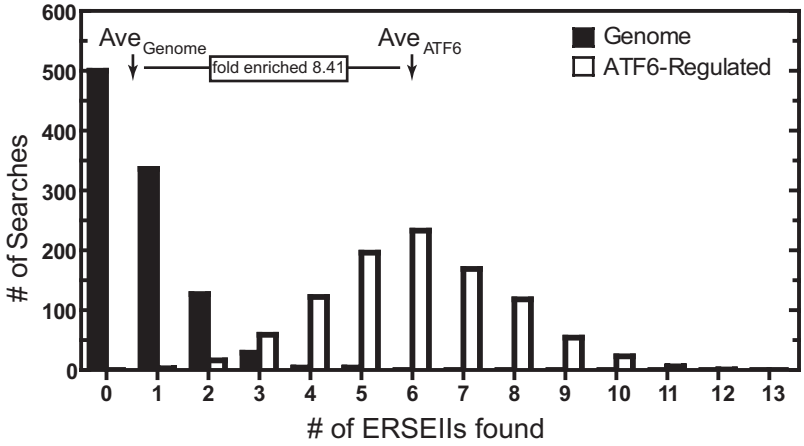

D ERSEII Totals

# of ERSEIIs Found	Genome Searches	ATF6-Regulated Searches
0	500	0
1	336	3
2	127	16
3	29	59
4	4	122
5	4	196
6	0	233
7	0	169
8	0	118
9	0	54
10	0	23
11	0	6
12	0	1
13	0	0
Ave # of ERSEIIs found:	0.71	6.00

Fold Enrichment: 8.41

E UPRE

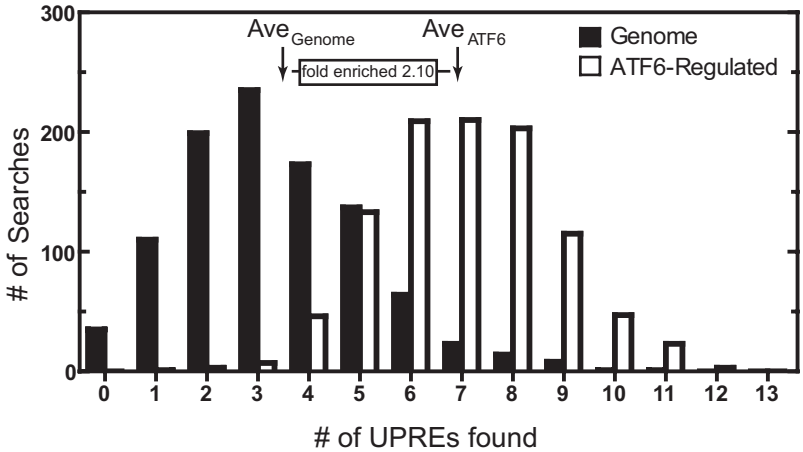

F UPRE Totals

# of UPREs Found	Genome Searches	ATF6-Regulated Searches
0	35	0
1	110	1
2	199	3
3	235	7
4	173	46
5	137	133
6	64	209
7	23	210
8	14	203
9	8	115
10	1	47
11	1	23
12	0	3
13	0	0
Ave # of UPREs found:	3.34	7.02

Fold Enrichment: 2.10

Figure 1. ATF6-MER TG mouse microarray is enriched in genes with ERSEs, ERSE-IIs, and/or UPREs. To determine the enrichment of the numbers of ERSEs in the ATF6-regulated gene list, a bootstrapping analysis was performed, as described in Methods. The number of times these elements were found in each search was plotted as a function of the number of searches, resulting in a representation of the frequency with which each was found in the whole genome (A, C, and E, black bars) and in the ATF6-regulated gene list (A, C, and E, white bars). The data used to generate each bar graph are shown in the tables in B, D, and F. For example, 417 of 1000 searches of the whole genome resulted in the identification of zero ERSEs (row 1, B). The average number of times each element was found per search (ie, average frequency) is shown as Ave_{Genome} and Ave_{ATF6}. The average frequency with which each element was found in the ATF6-regulated gene list was divided by the average in whole genome, and defined as the fold enrichment of the array.

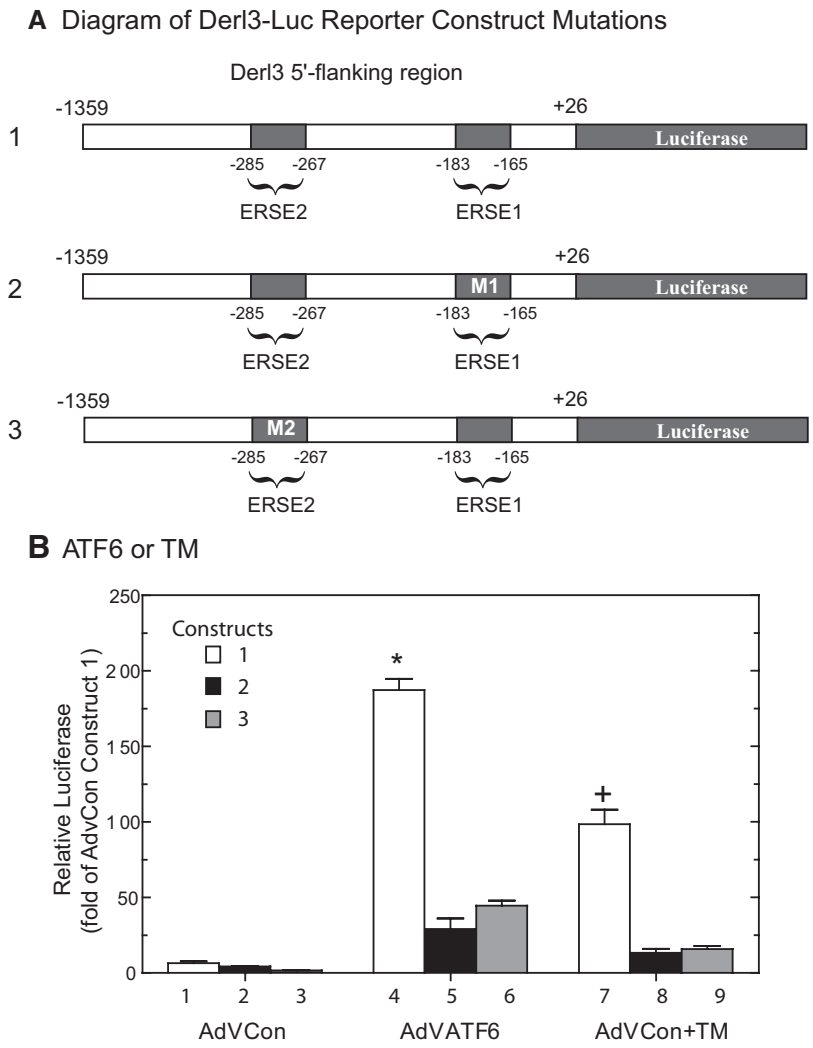

Figure 2. Effect of ATF6 overexpression and tunicamycin on Derl3 promoter activity in cultured cardiac myocytes. A, The mouse Derl3 promoter (−1359 to +26, construct 1) and versions harboring mutations in putative ERSE elements located at either −183 to −165 (construct 2) or −285 to −267 (construct 3) were cloned into a luciferase expression construct. B, NRVMCs were transfected with luciferase constructs 1, 2, or 3 and CMV-β-gal and then infected with AdV-Con or AdV-ATF6, as previously described.[19] Twenty-four hours after infection, cultures were treated with or without TM; 16 hours later, cultures were extracted and luciferase and β-galactosidase reporter enzyme activities were determined, as previously described.[19] Shown are the mean relative luciferase activities (luciferase/β-galactosidase), expressed as the fold of construct 1 treated with AdVCon (bar 1)±SE for each treatment (n=3 cultures per treatment, sum of 3 separate experiments). *$P \leq 0.05$, +$P \leq 0.05$ from all other values by ANOVA.

shown). In contrast, tamoxifen-treated ATF6-MER TG mouse hearts exhibited robust Derl3 expression that colocalized primarily with actin-positive cardiomyocytes (Figure 3C, overlay). Thus, ATF6 induces Derl3 expression in cardiac myocytes, in vivo.

Derl3 Is an ATF6-Inducible ER Stress Response Gene

The effects of ATF6 or ER stress on Derlin mRNA in cultured cardiac myocytes were examined. Derl3 was the only family member that exhibited ATF6-inducibility, in cultured cardiac myocytes (Figure 4A, bars 1 through 6). When cells were treated with TM, Derl1 and Derl2 mRNA levels were 3- and 8-fold of control, respectively (Figure 4B, bars 2 and 6); however, neither was affected by dominant-negative ATF6 (Figure 4B, bars 4 and 8). In contrast, on TM treatment, Derl3 mRNA was 200-fold of control (Figure 4B, bar 10), and this induction was attenuated by more than half by dominant-negative ATF6 (Figure 4B, bar 12).

Simulating ischemia (sI) activates ER stress in cardiac myocytes[19]; accordingly, the effect of sI on Derlin expression was examined. Whereas Derl1 and Derl2 have been shown to be inducible by TM in XBP1 knockout MEFs,[18] in the present study in NRVMCs, sI had no effect on Derl1, and Derl2 was only slightly increased, but this increase did not reach significance (Figure 4C, bars 2 and 6). In contrast, sI significantly increased Derl3 to ≈2.5-fold of control (Figure 4C, bar 10); moreover, sI-mediated Derl3 induction was completely blocked by dominant-negative ATF6 (Figure 4C, bar 12), which was different than the partial blockage of Derl3 induction following TM treatment. This could be attributable to the higher dynamic range of induction experienced with TM or attributable to other potential mediators of Derl3 induction during TM but not sI. Thus, Derl1 and Derl2 were induced by the prototypical ER stressor, TM, independently of ATF6. Moreover, only Derl3 was induced by the physiological ER stressor, sI, in an ATF6-dependent manner.

ATF6 Is Activated and Derl3 Is Induced in an In Vivo Model of Myocardial Infarction

We previously showed that ER stress is activated in the mouse heart by myocardial infarction (MI).[19] During ER stress, full-length, 90-kDa ATF6 is converted to 50-kDa ATF6, which is an active transcription factor.[6,23] Accordingly, the effects of ischemia on ATF6 and Derl3 after MI were examined in vivo. An MI time course indicated that the

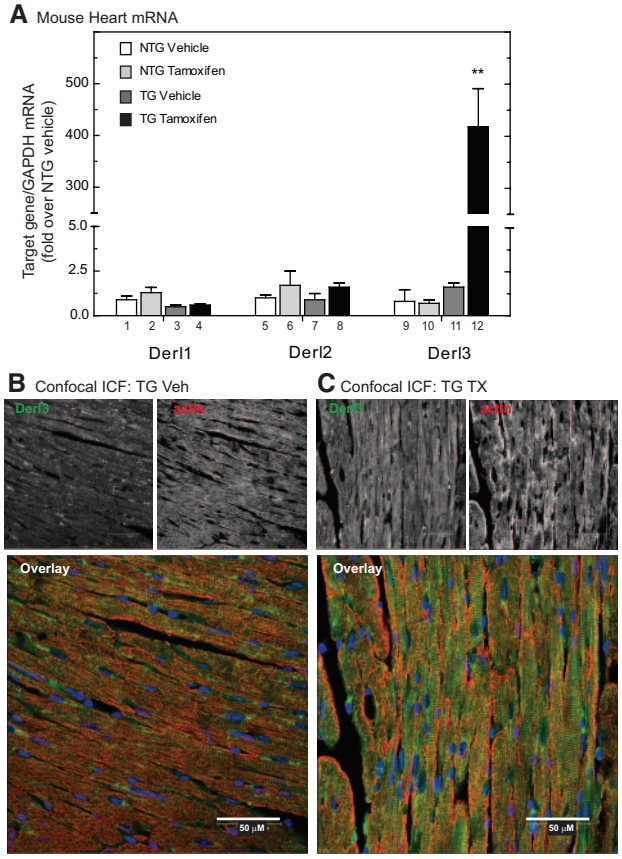

Figure 3. Effect of activated ATF6 on Derlin family member induction in ATF6-MER TG mouse hearts. A, NTG and ATF6-MER TG mice were treated with or without vehicle or tamoxifen, and RNA was extracted from hearts, as previously described.[14] RNA samples were subjected to quantitative RT-PCR (RT-qPCR) to examine the levels of mRNAs for Derl1, Derl2, Derl3, and GAPDH. Shown are the mean values of each target gene/GAPDH mRNA, expressed as the fold of NTG vehicle±SE for each target gene (n=3 mice per treatment). TG indicates ATF6-MER transgenic; Veh, vehicle; Tx, tamoxifen. $^{**}P \leq 0.01$ from all other values by ANOVA. B and C, TG mice were treated with vehicle (B) or tamoxifen (C), and hearts were sectioned for immunofluorescence confocal microscopy. Sections were costained with Derl3 and actin, as described in Methods.

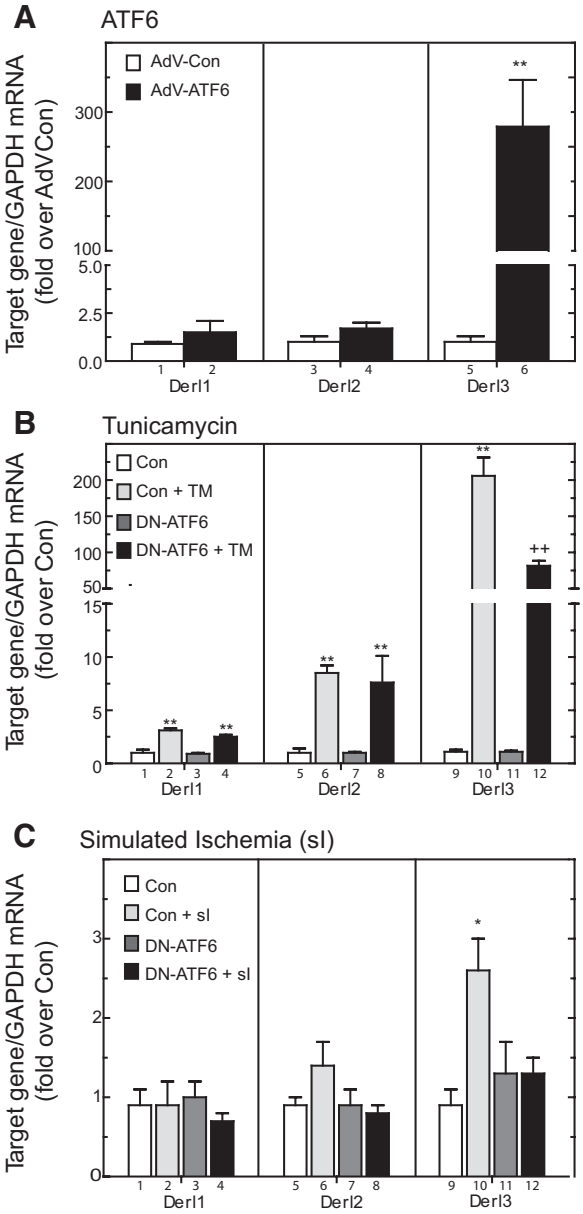

Figure 4. Derl3 mRNA is induced by ATF6 and TM in cultured cardiac myocytes. A, NRVMCs were infected with either AdV-Con or AdV-ATF6 (n=3 cultures per treatment). Forty-eight hours after infection, cultures were extracted and the RNA was subjected to RT-qPCR to examine the levels of mRNA for the target genes described in Figure 3. Shown are the means±SE for each target gene (n=3 cultures per treatment). $^{*}P \leq 0.05$ different from all other values by ANOVA. B and C, NRVMCs were infected with either AdV-Con or AdV-DNATF6 (n=3 cultures per treatment). Twenty-four hours after infection, cultures were treated with TM for 16 hours (10 mg/mL) (B) or sI for 20 hours (C). Cells were extracted and subjected to RT-qPCR to examine the levels of mRNA for the target genes described in A. Shown are the means±SE for each target gene (n=3 cultures per treatment).

50-kDa form of ATF6 increased significantly after 16 hour of MI, remained elevated after 1 day and 3 days and decreased at 4 days of MI, consistent with activation of ATF6 (Figure 5A and 5B).[24] The 50-kDa band migrated slightly further than a 3xFlag-tagged form of cleaved, N-terminal ATF6, consistent with its identity as cleaved ATF6 (Online Figure I, A).

The mRNA levels of all Derl family members increased in 4 days MI mouse hearts, compared to sham, with Derl1 and Derl3 reaching significance and Derl3 exhibiting the most robust upregulation of ≈6-fold (Figure 5C, bars 2, 4, and 6). An MI time course showed that although Derl3 mRNA showed a trend of being increased after 1 day MI, it was significantly increased after 4 days and 7 days of MI (Online Figure I, B; Online Data Supplement). The increase in p50 ATF6 by 16 hours of MI and continued elevation after 1 and 3 days of MI were consistent with the possibility that ATF6 could induce Derl3 mRNA as early as 1 day after MI. However, because the elevation of p50 ATF6 after 1 and 3 days of MI, and the elevated Derl3 mRNA after 1 day of MI did not reach statistical significance, it is formally possible that ATF6 activation/inactivation may precede Derl3 induction, suggesting that ATF6 may induce Derl3 expression indirectly. For example, ATF6 is known to induce the ER stress response transcription factor, XBP1, which could

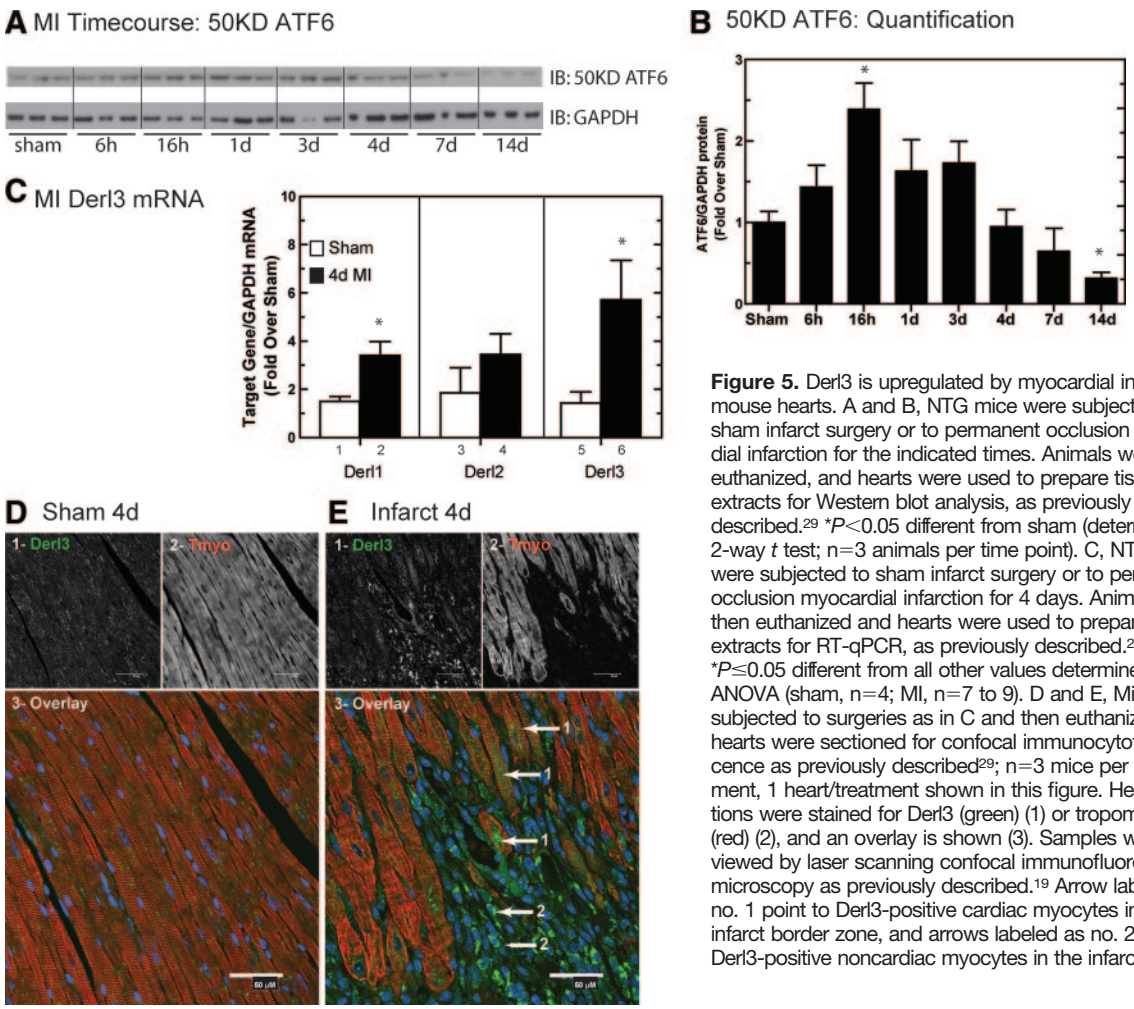

Figure 5. Derl3 is upregulated by myocardial infarction in mouse hearts. A and B, NTG mice were subjected to sham infarct surgery or to permanent occlusion myocardial infarction for the indicated times. Animals were euthanized, and hearts were used to prepare tissue extracts for Western blot analysis, as previously described.[29] *$P<0.05$ different from sham (determined by 2-way *t* test; n=3 animals per time point). C, NTG mice were subjected to sham infarct surgery or to permanent occlusion myocardial infarction for 4 days. Animals were then euthanized and hearts were used to prepare tissue extracts for RT-qPCR, as previously described.[29] *$P\leq0.05$ different from all other values determined by ANOVA (sham, n=4; MI, n=7 to 9). D and E, Mice were subjected to surgeries as in C and then euthanized, and hearts were sectioned for confocal immunocytofluorescence as previously described[29]; n=3 mice per treatment, 1 heart/treatment shown in this figure. Heart sections were stained for Derl3 (green) (1) or tropomyosin (red) (2), and an overlay is shown (3). Samples were viewed by laser scanning confocal immunofluorescent microscopy as previously described.[19] Arrow labeled as no. 1 point to Derl3-positive cardiac myocytes in the infarct border zone, and arrows labeled as no. 2 point to Derl3-positive noncardiac myocytes in the infarct zone.

induce Derl3. These limitations leave open the question of whether ATF6 directly induces Derl3 mRNA in the heart, which we intend to investigate in future studies; nonetheless, ATF6 is a potent inducer of Derl3 gene expression in the myocardium.

Derl3 was low in sham mouse hearts (Figure 5D, image 1) but elevated in surviving myocytes in the infarct zone (Figure 5E, images 1 and 3, arrow 1), as well as other tropomyosin-negative cells, which were most likely nonmyocytes (Figure 5E, images 1 and 3, arrow 2). Derl3 staining was perinuclear in the myocytes, consistent with expression in the ER.

Derl3 Protects Cardiac Myocytes From Cell Death

ERAD reduces ER stress by degrading misfolded ER proteins; accordingly, the effect of Derl3 on ER stress was examined. Following sI or simulated ischemia/reperfusion (sI/R), control cells exhibited a significant increase in the prototypical ER stress response proteins glucose-regulated protein (GRP)94 and GRP78 (Figure 6A, lanes 1 through 3 versus 7 through 9 and 11 through 13; Figure 6B and 6C, bars 1, 3, and 5). In contrast, cells infected with AdV-Derl3 exhibited reduced GRP94 and GRP78 (Figure 6A, lanes 4 through 6, 10 through 12 and 14 through 16; Figure 6B and 6C, bars 2, 4, and 6). GRP94 and GRP78 mRNA levels were also assessed following sI and sI/R (Online Figure II, A and B). Because neither GRP94 nor GRP78 mRNA levels were elevated following 20 hours of sI (Online Figure II, A and B, bars 3 through 4), we hypothesized that these mRNAs were increased at shorter times of sI. As indicated in Online Figure II (C and D), GRP94 and GRP78 mRNAs increased at shorter times of sI, reaching a maximum at 12 hours, and AdV-Derl3 reduced the induction seen at these sI time points, consistent with the reduced levels of these proteins following sI seen in Figure 6A through 6C. In addition, sI/R significantly increased GRP78 and GRP94 mRNA in AdVCon infected cells by ≈15 and 17 fold, respectively (Online Figure II, A and B, bar 5). AdV-Derl3–infected cells exhibited a significant reduction in sI/R-mediated GRP78 and GRP94 mRNA (Online Figure II, A and B, bar 5 versus 6). Together, these results suggest that overexpression of Derl3 attenuated sI- and sI/R-activated ER stress.

Prolonged ER stress activates apoptosis[6,23,25,26]; accordingly, we assessed whether Derl3 overexpression decreased the ER stress-inducible, proapoptotic protein, C/EBP homologous protein (CHOP) and caspase-3 activation. AdV-Con cells exhibited ≈25- and 5-fold increase in CHOP following sI and sI/R, respectively (Figure 6D, lanes 1 and 2 versus 5 and 6 and 9 and 10; Figure 6E, bars 1, 3, and 5). In contrast, AdV-Derl3 cells exhibited decreased CHOP induction fol-

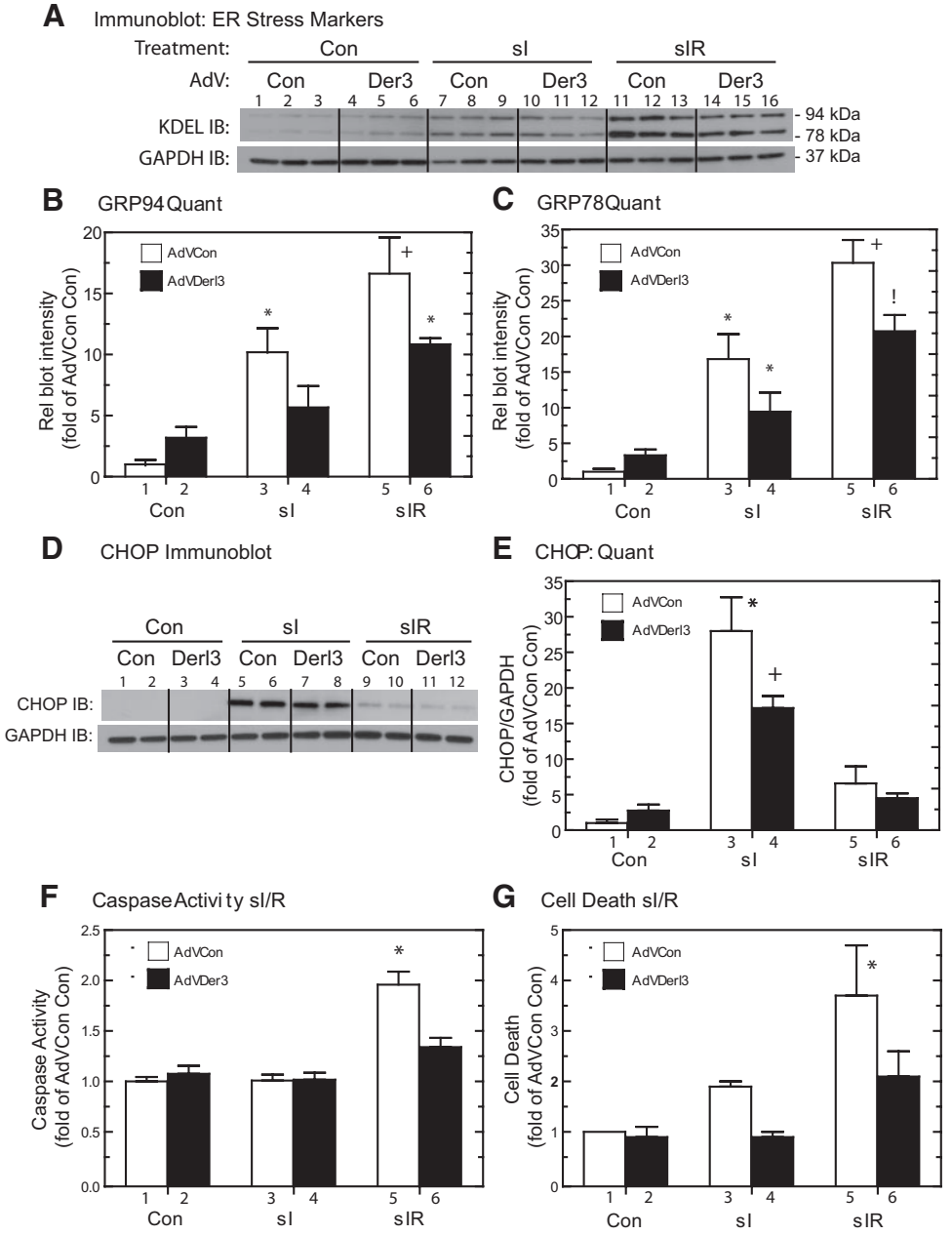

Figure 6. Derl3 overexpression attenuates ER stress activation, caspase activity, and cell death following sI and/or sI/R. A through C, NRVMCs were infected with or without AdV-Con or AdV-Derl3, and 24 hours later, cultures were treated with or without sI or sI/R. Cultures were then extracted, and cell lysates were analyzed for the levels of the prototypical ERSR proteins GRP78 and GRP94 using an anti-KDEL antibody (A), as previously described. B and C, Relative blot intensities of each protein/GAPDH, expressed as the fold of control (bar 1)±SE for each treatment (n=3 cultures per treatment). D and E, NRVMCs were treated as in A, and cultures were extracted and analyzed for the levels of CHOP using an anti-CHOP antibody in D and quantified in E. F, NRVMCs were treated as in A. Cultures were then assayed for caspase-3 activation, as described in Methods. G, NRVMCs were treated as in A. Cultures were then stained with Hoechst and propidium iodide (PI), and images of 5 randomly chosen fields per culture were viewed at ×10 magnification on a fluorescent microscope. The numbers of Hoechst-positive (total) cells and PI-positive (dead) cells were then quantified using NIH ImageJ software (n=3 cultures per treatment, sum of 3 separate experiments). Shown is the relative amount of cell death, expressed as fold of AdVCon Con±SE for each treatment. *$P \leq 0.05$, +$P \leq 0.05$, !$P \leq 0.05$ different from all other values by ANOVA.

lowing sI and sI/R (Figure 6D, lanes 3 and 4, 7 and 8, and 11 and 12; Figure 6E, bars 2, 4, and 6). sI did not activate caspase-3 in AdV-Con– or AdV-Derl3–infected cells, which is consistent with the lack of ATP required to activate caspase during sI (Figure 6F, bars 1 and 2 versus 3 and 4). However, sI/R resulted in a ≈2-fold increase in caspase-3 in AdV-Con–infected cells, which was attenuated in AdV-Derl3–infected cells (Figure 6F, bars 5 and 6). In addition, AdV-Con–infected cells exhibited a ≈2-fold and 3.5-fold increases in cell death following sI and sI/R, respectively (Figure 6G, bars 1 versus 3 and 5). In contrast, AdV-Derl3–infected cells exhibited significantly less cell death in response to sI/R (Figure 6G, bar 6). Thus, overexpression of Derl3 attenuated ER stress and apoptosis in cardiac myocytes subjected to these stressors.

Derl3 Enhances ERAD and Reduces ER Stress

The effect of Derl3 on ERAD was examined using a mutant form of the α-1 anti-trypsin protein (A1ATmut), which is constitutively misfolded in the ER.[27] HeLa cells were cotransfected with plasmids expressing A1ATmut and Derl3-encoding plasmid. Derl3 overexpression decreased A1ATmut (Figure 7A and 7B), indicating that Derl3 augmented clearance of misfolded proteins in the ER during ERAD.

The effect of A1ATmut overexpression on ER stress was determined by measuring GRP78 promoter activation. Cells were transfected with plasmids expressing a GRP78-luciferase promoter and A1ATwt, which folds properly or A1ATmut. Whereas A1ATwt had no effect, promoter activity was ≈2-fold of control in cells transfected with A1ATmut (Figure 7C, bars 2 and 3). Moreover, cotransfecting Derl3

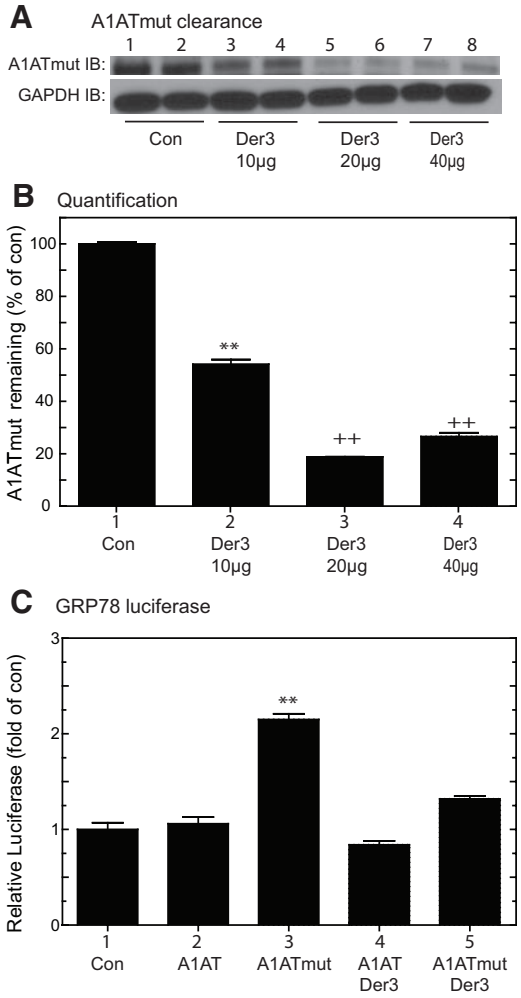

Figure 7. Derl3 overexpression enhances misfolded protein clearance and attenuates ER stress activation. A and B, HeLa cells were cotransfected with plasmids encoding A1ATmut, along with either an empty vector or increasing concentrations of a plasmid expressing Derl3. Forty-eight hours later, cultures were extracted, and lysates were analyzed for A1ATmut by immunoblot. Shown are the relative blot intensities of A1ATmut/GAPDH, expressed as the fold of control (bar 1)±SE for each treatment (n=3 cultures per treatment). $^{**}P \leq 0.01$, $++P \leq 0.01$ different from all other values by ANOVA. C, NRVMCs were transfected with a GRP78 promoter/luciferase construct and CMV-β-gal as described previously,[19] along with plasmids encoding A1ATwt or A1ATmut and Derl3. Forty-eight hours later, cells were extracted and luciferase and β-galactosidase reporter enzyme activities were determined, as previously described.[19] Shown are the mean relative luciferase (luciferase/β-galactosidase), expressed as the fold-of-control (bar 1)±SE for each treatment (n=3 cultures per treatment, sum of 3 separate experiments). $^{**}P \leq 0.01$ different from all other values by ANOVA.

decreased A1ATmut-mediated GRP78 promoter activation (Figure 7C, bars 3 versus 5). Thus, Derl3 enhanced the removal of A1ATmut and, in so doing, decreased ER stress.

Dominant Negative Derl3 and microRNA Directed to Derl3 Enhance sI/R-Mediated Cardiac Myocyte Death

An expression construct encoding an inactive, dominant-negative (DN) form of Derl3 was designed based on previous studies using Derl1 and 2 DN constructs.[17] HeLa cells were transfected with A1ATmut, control, Derl3, or Derl3-DN plasmids. Derl3 conferred an approximate 70% reduction in the level of A1ATmut, whereas Derl3-DN did not significantly change the levels of A1ATmut (Figure 8A and 8B). Thus, unlike wild-type Derl3, Derl3-DN does not increase the clearance of A1ATmut.

Cultured cardiac myocytes were transfected with Derl3-DN, subjected to sI or sI/R, and then analyzed for cell death by flow cytometry. Compared to control, cells transfected with Derl3-DN exhibited slight increases in cell death under control conditions, although this did not reach significance (Figure 8C, bars 1 versus 2). Cells transfected with Derl3-DN exhibited significant increases in cell death on sI and sI/R (Figure 8C, bars 3 versus 4 and 5 versus 6).

To examine roles for Derl3 on cell survival, recombinant adenovirus encoding Derl3-targeted microRNA (miRNA) (AdVmiDerl3) was generated. Compared to control, AdVmiDerl3 decreased basal Derl3 mRNA levels by ≈70% (Figure 8D). To determine whether sI increased Derl3 protein, and whether AdVmiDerl3 could attenuate this increase, NRVMCs were treated with AdVmiDerl3, subjected to sI, and lysates were examined for Derl3 protein. Derl3 was increased with sI (Figure 8E, bars 1 through 3 versus 4 through 6; Figure 8F, bars 1 versus 2). This increase was significantly attenuated by AdVmiDerl3 (Figure 8E, lanes 4 through 6 versus 10 through 12; Figure 8F, bars 2 versus 4). AdVmiDerl3 slightly increased cell death under basal conditions, although this increase did not reach significance (Figure 8G, bars 1 versus 2); however, compared to control, AdVmiDerl3 significantly increased cell death during sI (Figure 8G, bars 3 versus 4) and sI/R (Figure 8G, bars 5 versus 6).

Thus, Derl3-DN or Derl3 knockdown attenuated clearance of misfolded ER proteins, and augmented sI and sI/R-mediated cell death, suggesting that the ability to clear misfolded proteins from the ER is especially critical during ischemic stress.

Discussion

ER stress is activated in the heart during ischemia and that ATF6 protects the heart from ischemic damage, in vivo. ATF6 induces numerous known and novel ER stress response genes, however, only recently have potential ATF6 gene targets been identified in the heart[15]; however, it is unclear which genes contribute to myocardial protection. In the present study, a detailed promoter analysis identified 16 ATF6-regulated genes which contained canonical ATF6-binding elements (Online Tables I through III). Only 2 of these genes contain 2 canonical ER stress response elements: GRP94, the well-known ER stress responsive chaperone; and Derl3, which encodes a protein likely to be involved in ERAD. Neither Derl3 nor the functional consequences of ERAD have been studied in the cardiac context; therefore, the present study focused on this gene and roles for ERAD in cultured cells and in the mouse heart, in vivo.

The Derlins are all ER transmembrane proteins that associate with other proteins that participate in the degradation of misfolded proteins in the ER. Derl1 and Derl2 associate with

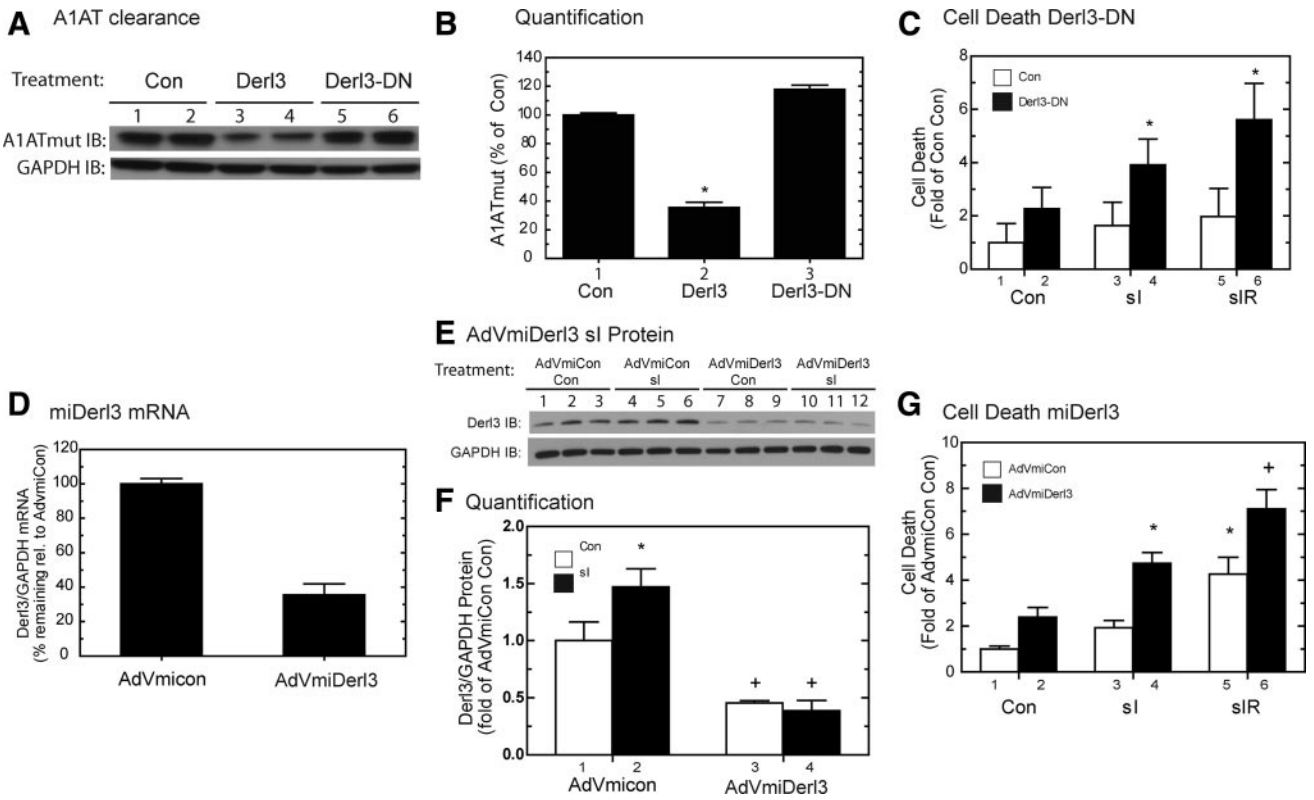

Figure 8. Overexpression of Derl3-DN attenuates misfolded protein clearance and enhances cell death. A and B, HeLa cells were transfected with plasmids encoding A1ATmut along with either green fluorescent protein (GFP), Derl3, or Derl3-DN. Forty-eight hours after transfection, cells were extracted and analyzed for A1ATmut levels by immunoblot. Shown are the relative blot intensities of A1ATmut/GAPDH, expressed as the fold of control (bar 1)±SE for each treatment (n=3 cultures per treatment, sum of 3 separate experiments). C, NRVMCs were transfected with plasmids encoding GFP alone or Derl3-DN, which encodes a Derl3-GFP fusion protein. Twenty-four hours after transfection, cultures were subjected to sI or sI/R, after which cells were collected and analyzed by flow cytometry. Cells were gated for GFP expression to identify transfected cells, and then the transfected cells were assessed for cell death by PI incorporation, as described in Methods. The gate for GFP fluorescence intensity was established by comparing both groups of transfected cells to nontransfected, naïve cells. The same GFP intensity gate was used for the cells transfected with the control plasmid, as well as those transfected with Derl3-DN. Shown are the percentage of GFP-positive cells that are positive for PI, expressed as fold of control (bar 1) (±SE, n=3 cultures per treatment, sum of 3 separate experiments). *$P \leq 0.05$ different from all other values by ANOVA. D, NRVMCs were infected with either an adenovirus encoding a nonspecific miRNA (AdVmiCon) or an miRNA directed to Derl3 (AdVmiDerl3). Forty-eight hours after infection, cultures were extracted and the RNA was subjected to RT-qPCR to examine the levels of Derl3 mRNA. Shown are the means±SE for each target gene (n=3 cultures per treatment). *$P \leq 0.05$ different from AdVmiCon by 2-way *t* test. E and F, NRVMCs were infected as in D and 24 hours later, cultures were treated±sI. Cells were lysed and analyzed for Derl3 protein levels as described in Methods (n=3 cultures per treatment, sum of 2 separate experiments). Shown is the relative amount of Derl3 protein, expressed as fold of AdVCon Con±SE for each treatment. *$P \leq 0.05$, +$P \leq 0.05$ different from all other values by ANOVA. G, NRVMCs were infected as in D, and 24 hours later, cultures were treated with or without sI or sI/R. Cultures were then stained with Hoechst and PI and analyzed for cell death as in Figure 6G (n=3 cultures per treatment, sum of 3 separate experiments). Shown is the relative amount of cell death, expressed as fold of AdVCon Con±SE for each treatment. *$P \leq 0.05$, +$P \leq 0.05$ different from all other values by ANOVA.

the p97 AAA ATPase and VIMP,[17] Derl2, and Derl3 associate with proteins known to be involved in ERAD, EDEM, and p97,[18] and the Derl3 yeast homolog Der3p/Hrd1p interacts with Hrd3p and the retro-translocon pore complex protein Sec61p.[28] Overexpression of Derl2 and Derl3 accelerates degradation of known misfolded substrates in HEK293 cells, whereas knockdown blocks degradation.[18] In addition, the IRE1/XBP1 pathway was implicated to play a role in induction of Derl1 and Derl2; however, the specific mechanism of Derl3 induction was not determined.[18]

In the present study, it was shown that Derl3 was strongly induced by ATF6 in vivo, a finding that was replicated in cultured cardiac myocytes. Derl3 was also induced in the infarct border zone in an in vivo mouse model of myocardial infarction and by simulated ischemia in cultured cardiac myocytes.

Because Derl3 enhances ER-associated degradation of misfolded proteins in other cell types, we investigated the possibility that Derl3 may serve a potentially beneficial role during physiologically relevant stresses in cardiac myocytes, such as ischemia and/or reperfusion. We found that overexpressing Derl3 attenuated long-term ER stress response signaling and cell death in response to sI and sI/R, suggesting that enhancing elements of the ERAD machinery in the heart can protect from ischemic injury. Although the present study indicates that Derl3 is induced in the heart, in vivo, by physiological stress, such as myocardial infarction, additional studies must be carried out using overexpression or knockdown of Derl3 or other ERAD components, in vivo, to determine whether enhancing or inhibiting ERAD in the heart can result in attenuation or exacerbation of ischemic damage in cardiac tissue.

Sources of Funding

This work was supported by NIH grants HL-075573 and HL-085577. P.J.B. and N.G. are fellows of the Rees-Stealy Research Foundation and the San Diego State University Heart Institute. P.J.B. is a scholar of the San Diego Chapter of the Achievement Rewards for College Scientists (ARCS) Foundation and a recipient of an American Heart Association Western States Affiliate Predoctoral Fellowship (Award 0815210F). M.N.S.P. is a Minority Access to Research Careers (MARC) scholar and a recipient of a MARC fellowship (NIH/NIGMS SDSU MARC 5T34 GM08303).

Disclosures

None.

References

1. Szegezdi E, Duffy A, O'Mahoney ME, Logue SE, Mylotte LA, O'Brien T, Samali A. ER stress contributes to ischemia-induced cardiomyocyte apoptosis. *Biochem Biophys Res Commun*. 2006;349:1406–1411.
2. Kaufman RJ. Orchestrating the unfolded protein response in health and disease. *J Clin Invest*. 2002;110:1389–1398.
3. Aridor M. Visiting the ER: the endoplasmic reticulum as a target for therapeutics in traffic related diseases. *Adv Drug Deliv Rev*. 2007;59:759–781.
4. Wang X, Osinska H, Klevitsky R, Gerdes AM, Nieman M, Lorenz J, Hewett T, Robbins J. Expression of R120G-alphaB-crystallin causes aberrant desmin and alphaB-crystallin aggregation and cardiomyopathy in mice. *Circ Res*. 2001;89:84–91.
5. Pattison JS, Sanbe A, Maloyan A, Osinska H, Klevitsky R, Robbins J. Cardiomyocyte expression of a polyglutamine preamyloid oligomer causes heart failure. *Circulation*. 2008;117:2743–2751.
6. Glembotski CC. The role of the unfolded protein response in the heart. *J Mol Cell Cardiol*. 2008;44:453–459.
7. Lee AS. Mammalian stress response: induction of the glucose-regulated protein family. *Curr Opin Cell Biol*. 1992;4:267–273.
8. Shamu CE, Cox JS, Walter P. The unfolded-protein-response pathway in yeast. *Trends Cell Biol*. 1994;4:56–60.
9. McMillan DR, Gething MJ, Sambrook J. The cellular response to unfolded proteins: intercompartmental signaling. *Curr Opin Biotechnol*. 1994;5:540–545.
10. Nakatsukasa K, Huyer G, Michaelis S, Brodsky JL. Dissecting the ER-associated degradation of a misfolded polytopic membrane protein. *Cell*. 2008;132:101–112.
11. Razeghi P, Taegtmeyer H. Cardiac remodeling: UPS lost in transit. *Circ Res*. 2005;97:964–966.
12. Wang X, Robbins J. Heart failure and protein quality control. *Circ Res*. 2006;99:1315–1328.
13. Yamamoto K, Yoshida H, Kokame K, Kaufman RJ, Mori K. Differential contributions of ATF6 and XBP1 to the activation of endoplasmic reticulum stress-responsive cis-acting elements ERSE, UPRE and ERSE-II. *J Biochem*. 2004;136:343–350.
14. Martindale JJ, Fernandez R, Thuerauf D, Whittaker R, Gude N, Sussman MA, Glembotski CC. Endoplasmic reticulum stress gene induction and protection from ischemia/reperfusion injury in the hearts of transgenic mice with a tamoxifen-regulated form of ATF6. *Circ Res*. 2006;98:1186–1193.
15. Belmont PJ, Tadimalla A, Chen WJ, Martindale JJ, Thuerauf DJ, Marcinko M, Gude N, Sussman MA, Glembotski CC. Coordination of growth and endoplasmic reticulum stress signaling by regulator of calcineurin 1 (RCAN1), a novel ATF6-inducible gene. *J Biol Chem*. 2008;283:14012–14021.
16. Hiller MM, Finger A, Schweiger M, Wolf DH. ER degradation of a misfolded luminal protein by the cytosolic ubiquitin-proteasome pathway. *Science*. 1996;273:1725–1728.
17. Lilley BN, Ploegh HL. Multiprotein complexes that link dislocation, ubiquitination, and extraction of misfolded proteins from the endoplasmic reticulum membrane. *Proc Natl Acad Sci U S A*. 2005;102:14296–14301.
18. Oda Y, Okada T, Yoshida H, Kaufman RJ, Nagata K, Mori K. Derlin-2 and Derlin-3 are regulated by the mammalian unfolded protein response and are required for ER-associated degradation. *J Cell Biol*. 2006;172:383–393.
19. Thuerauf DJ, Marcinko M, Gude N, Rubio M, Sussman MA, Glembotski CC. Activation of the unfolded protein response in infarcted mouse heart and hypoxic cultured cardiac myocytes. *Circ Res*. 2006;99:275–282.
20. Yoshida H, Haze K, Yanagi H, Yura T, Mori K. Identification of the cis-acting endoplasmic reticulum stress response element responsible for transcriptional induction of mammalian glucose-regulated proteins. Involvement of basic leucine zipper transcription factors. *J Biol Chem*. 1998;273:33741–33749.
21. Kokame K, Kato H, Miyata T. Identification of ERSE-II, a new cis-acting element responsible for the ATF6-dependent mammalian unfolded protein response. *J Biol Chem*. 2001;276:9199–9205.
22. DenBoer LM, Hardy-Smith PW, Hogan MR, Cockram GP, Audas TE, Lu R. Luman is capable of binding and activating transcription from the unfolded protein response element. *Biochem Biophys Res Commun*. 2005;331:113–119.
23. Glembotski CC. Endoplasmic reticulum stress in the heart. *Circ Res*. 2007;101:975–984.
24. Thuerauf DJ, Morrison L, Glembotski CC. Opposing roles for ATF6alpha and ATF6beta in endoplasmic reticulum stress response gene induction. *J Biol Chem*. 2004;279:21078–21084.
25. Oyadomari S, Koizumi A, Takeda K, Gotoh T, Akira S, Araki E, Mori M. Targeted disruption of the Chop gene delays endoplasmic reticulum stress-mediated diabetes. *J Clin Invest*. 2002;109:525–532.
26. Austin RC. The unfolded protein response in health and disease. *Antioxid Redox Signal*. In press.
27. Sifers RN, Brashears-Macatee S, Kidd VJ, Muensch H, Woo SL. A frameshift mutation results in a truncated alpha 1-antitrypsin that is retained within the rough endoplasmic reticulum. *J Biol Chem*. 1988;263:7330–7335.
28. Plemper RK, Egner R, Kuchler K, Wolf DH. Endoplasmic reticulum degradation of a mutated ATP-binding cassette transporter Pdr5 proceeds in a concerted action of Sec61 and the proteasome. *J Biol Chem*. 1998;273:32848–32856.
29. Tadimalla A, Belmont PJ, Thuerauf DJ, Glassy MS, Martindale JJ, Gude N, Sussman MA, Glembotski CC. Mesencephalic astrocyte-derived neurotrophic factor is an ischemia-inducible secreted endoplasmic reticulum stress response protein in the heart. *Circ Res*. 2008;103:1249–1258.

SUPPLEMENT MATERIAL

Expanded Materials and Methods:

Animals-

The transgenic mice used in this study have been described previously.[1] Approximately 100 neonatal rats and 24 adult male mice were used in this study. All procedures involving animals were in accordance with the San Diego State University Institutional Animal Care and Use Committee.

Promoter Searches-

The 2kb region lying 5' of the start sites for each of the ATF6-regulated transcripts identified in our previous array study[2] were retrieved using Ensembl Biomart (http://www.ensembl.org/biomart/martview). The same regions of each of the roughly 40,000 transcripts on the Affymetrix mouse 430 2.0 whole genome array chips (Affymetrix, Inc., part #900496) used in this previous study were also acquired. These sequences were then searched for ERSEs, ERSE-IIs and UPREs using a custom Perl script and the following sequences:

ERSE- CCAAT-N9-CCACG[3]
ERSE 1bp mismatch- Allows for 1bp mismatch in any nucleotide in either of the 5bp flanking regions of the consensus ERSE
ERSE-II- ATTGG-N-CCACG[4]
ERSE-II 1bp mismatch- Allows for 1bp mismatch in any nucleotide in either of the 5bp flanking regions of the consensus ERSEII
UPRE: TGACGTGGA[5]
UPRE 1bp mismatch: Allows for 1bp mismatch in any nucleotide of the consensus UPRE

Enrichment of ATF6 Array for Putative ER Stress Response Genes-

To determine whether the genes previously identified in the mouse heart as ATF6-regulated[2] were enriched for ERSEs, ERSE-IIs and UPREs, a bootstrapping analysis was performed, essentially as previously described.[6,7] Briefly, 1,000 promoter sets, each of which contains 607 promoters, were generated from genes either from the mouse whole-genome Affymetrix GeneChip array, or from the ATF6-regulated gene cluster, using Ensembl Biomart (http://www.ensembl.org/biomart/martview). Bootstrapped promoter sets were generated using a custom Perl script. The number of times these elements were found in each bootstrapped promoter set, i.e. the frequency of appearance in the whole genome and in the ATF6-regulated genes, is shown in **Figure 1**.

Cultured Cardiac Myocytes-

Primary neonatal rat ventricular myocyte cultures (NRVMC) were prepared and maintained in culture, as previously described.[8]

Derl3-luciferase and Derl3-mut-luciferase Constructs-

The mouse Derl3 gene from nt -1359 to +26 was amplified by PCR and cloned into a pGL2 luciferase reporter vector (Clontech, Inc.) and designated Construct 1. Two consensus ERSE sequences[5], CCAAT$(N)_9$CCACG, located between nt -183 to -165 and nt -285 to -267 were designated ERSE1 and ERSE2, respectively. Using PCR-based mutagenesis, ERSE1 of Derl3-luciferase Construct 1 was mutated to AACCG$(N)_9$AACAT, creating Construct 2. ERSE2 of Derl3-luciferase Construct 1 was also mutated to AACCG$(N)_9$AACAT, creating Construct 3.

Reporter Enzyme Assays-

Reporter enzyme assays for luciferase and β-galactosidase were carried out in NRVMC extracts as previously described.[8]

Simulated Ischemia/Simulated Reoxygenation-

NRVMCs were subjected to conditions that simulate ischemia (sI), or simulate ischemia followed by reoxygenation (sI/R), essentially as previously described.[8] Briefly, for sI, the medium was replaced with glucose-free DMEM/F12 containing 2% dialyzed fetal bovine serum and 3 mM 2-deoxyglucose (Sigma, catalog #D6134), and cultures were placed in a chamber (PROOX model 110, Sensor Part #E702, BioSpherix, Ltd Redfield, NY), filled with N_2/CO_2 (95% N_2/ 5% CO_2) for 20h. For sI/R, following sI, the medium was replaced with glucose-containing DMEM/F-12 supplemented with 2% bovine serum albumin, and cultures were incubated in O_2/CO_2 (18% O_2) for 24h. For immunoblot analysis, cells were lysed as previously described.[9] GRP78 and GRP94 protein levels were assessed using an anti-KDEL antibody (Stressgen, catalog # SPA-827); Derl3 protein levels were assessed using an anti-Derl3 antibody (LifeSpan Biosciences, catalog #LS-C80661).

Tamoxifen Treatment-

Non-transgenic (NTG) and transgenic (TG) mice were treated with vehicle or tamoxifen, n=3 mice per treatment group, and RNA was extracted from mouse heart ventricles, as described previously.[1]

Myocardial Infarction-

NTG mice were subjected to *in vivo* permanent myocardial infarction for 6h, 16h, 1d, 3d, 4d, 7d, or 14d. After each time point, mice were sacrificed and sections of the hearts were prepared for immunocytofluoescence confocal microscopy. Tissue extracts were also prepared for qRT-PCR or western blot analysis. All of these procedures have been previously described.[8,10] An antibody which recognizes cleaved, 50KD ATF6 was used (ATF6 H-280, Santa Cruz, catalog #22799).

Immunocytofluorescence-

Immunofluorescent confocal microscopy was carried out as previously described.[10] Sections were stained using an anti-Derl3 antibody (Sigma, catalog #D2194) at a dilution of 1:40.

Real Time Quantitative-PCR-

Real time quantitative-PCR (RT-qPCR) was performed, as previously described.[1] The following rat primer pairs were used:

Derl1: 5'-CTTAATGGCCGAGCTCTTGC; 3'-CATTCAGCGTGGGTCAGGT
Derl2: 5'-CTTTCTGCCCTGGGTGCTC; 3'-AATCGAGTTCCCCAGCAACA
Derl3: 5'-CCAGCAACACCATGCACTTC; 3'-TCACTGTGGTTGAGCGGAGA
GAPDH: 5;- CCTGGCCAAGGTCATCCAT; 3'- GTCATGAGCCCTTCCACGAT

The following mouse primer pairs were used:
Derl1: 5'-CTAATGTCCTGGTACCCGGC; 3'-CCCTTCGAAAAGCCAGTCCT
Derl2: 5'-ACCTTGCTTGTCTCGTTCAGC; 3'-AGACGTGATTGCAGACTTCGG
Derl3: 5'-GAGCAGGAAGCCCACTCTGA; 3'-GAGCTGAGGTGGAGGGAAGG
GAPDH: 5;- CCTGGCCAAGGTCATCCAT; 3'- GTCATGAGCCCTTCCACGAT

Plasmid Constructs-

3xFlag-ATF6- A plasmid encoding a 3xFlag-tagged version of the N-terminal portion of ATF6 (amino acids 1-373) has been constructed as previously described.[11]

α*-1Antitrypsin and Mutant* α*-1Antitrypsin*- A construct encoding human α-1 antitrypsin (A1AT, NCBI RefSeq NM_000295) was generated by PCR using the appropriate primers to create an amplicon with Xho1 on the 5' end of the start site, and a termination codon and EcoRI on the 3' end. This PCR product was cloned into the pCDNA3.1 vector. Mutant α-1 antitrypsin (A1ATmut) was generated by making a two nucleotide deletion at aa318 of A1AT, leading to a frameshift mutation, as previously described,[12] using PCR-based mutagenesis. Clones were generated using QuikChange from Stratagene and the appropriate primers.

Derl3-GFP Fusion Protein-

A construct encoding GFP fused to the C-terminus of Derl3 (Derl3-DN) was created by PCR, using mouse Derl3 (NCBI RefSeq NM_024440) as the template, and the appropriate primers, to create an amplicon with an Xho1 site on the 5'-end, and a termination codon and EcoRI site on the 3'-end. This PCR product was then cloned into the pEGFP-N1 vector (Clontech, catalog #6085-1, GenBank™ accession number U55762). Clones were generated using QuikChange from Stratagene and the appropriate primers.

Adenovirus-

Recombinant adenovirus (AdV) encoding only GFP (AdVCon), GFP and constitutively active ATF6 (AdVATF6), or GFP and dominant-negative ATF6 (AdVDN-ATF6), which encode proteins of the expected physical characteristics, were prepared as previously described [8]. A recombinant AdV encoding GFP and Derl3 (AdVDerl3) was generated by cloning a construct encoding mus Derl3 (NCBI RefSeq NM_024440) into the adenovirus shuttle vector, pAdTrack-CMV, and was used to create a new AdV strain, as previously described.[13] Recombinant AdV encoding GFP and A1AT (AdVA1AT) and GFP and mutA1AT (AdVmutA1AT) were generated by cloning constructs encoding human A1AT (NCBI RefSeq NM_000295) or mutA1AT, a mutated version of human A1AT, described above, into the adenovirus shuttle vector, pAdTrack-CMV, and used to create new AdV strains, as previously described.[13] Recombinant adenovirus encoding either miRNA targeted to rat Derl3 (AdVmiDerl3) or a negative control (AdVmiCon) were created using the Gateway System from Invitrogen, as previously described.[9]

Caspase-3 Activity Assay-

NRVMCs were infected with AdVCon vs AdVDerl3, or AdVmiCon vs AdVmiDerl3, in 2% FCS-containing medium for 6 hours, after which, cells were washed and fed with the same medium but without the AdV. After 24h, cells were treated +/- sI or sI/R, as described above. Cultures were extracted in caspase assay buffer containing 50 mM Hepes, pH 7.4, 0.1% CHAPS, 0.1 mM EDTA. A total of 50 μL of the lysate and 10 μL of the assay buffer were then combined with 45 μL of reaction buffer (40 μL caspase assay buffer, 1 mM DTT, 40 μM DEVD-AFC in DMSO (Sigma, catalog no. A0466). After 1 hour at 37°C, fluorescence was measured at an excitation wavelength of 400 nm and an emission wavelength of 505 nm. Caspase activity was defined as fluorescence/protein.

Live/Dead Assay-

Assessment of cell death in NRVMCs was performed using Hoescht (catalog no. H21486; Invitrogen) and propidium iodide (PI, Invitrogen, catalog no. P1304MP), as previously described.[10]

Protein Clearance Assays-

HeLa cells were co-transfected with A1ATmut and varying concentrations of Derl3, or co-transfected with A1ATmut and GFP or Derl3-DN. After 24h, cultures were scraped in protein lysis buffer, and immunoblotted with anti-A1AT antibody (Dako, Denmark A/S, Catalog #A 0012).

Flow Cytometry-

NRVMCs were electroporated with plasmids encoding GFP alone or Derl3-DN, which encodes a Derl3-GFP fusion protein, and plated onto 6-well dishes. Cultures were subjected to sI or sI/R, as described above. Cells were then collected using TripLE (Gibco, catalog #12605), washed with PBS, resuspended in PBS, and analyzed by flow cytometry on a BD FACSAria^{TM} cell sorter. Approximately 150,000 events were recorded for each condition. Cells were first gated to eliminate debris and aggregates. Transfected cells were identified by gating for GFP expression, and the percentage of these transfected cells that were also PI-positive was determined. This percentage was normalized to the percent of overall PI-positive cells for each condition. Data is presented as fold of control. Shown is the average of three independent experiments.

Statistical Analyses-

Data are reported as mean ± SEM and analyzed via 1-way ANOVA with Newman–Keuls post-hoc analysis using SPSS version 11.0. Unless otherwise stated in the figure legends, *, +, #, or ! = $p \leq 0.05$ different from all other values, and **, ++ = $p \leq 0.01$ different from all other values.

Supplemental Table Legends

Online Table I. Genes containing consensus ERSE elements within 2KB promoter regions.

Each unique gene containing a consensus ERSE (CCAAT-N9-CCACG) is numbered once. All ATF6-regulated genes are sorted by the fold change from our previous array study.[2] All genes from the full genome are sorted alphabetically. The MGI symbol, alias or common name, and NCBI Reference Sequence ID, or accession number, is shown for each gene. More information about each gene can be obtained by entering the MGI symbol into the Mouse Genome Informatics (MGI 3.54) web site. Also shown is the Start and End location for each ERSE identified, as determined by retrieving the 2000bp 5' flanking promoter sequence using Ensembl Biomart (http://www.ensembl.org/biomart/martview) and searching for each element with our custom Perl script.

Online Table II. Genes containing consensus ERSEII elements within 2KB promoter regions.

Each unique gene containing a consensus ERSEII (ATTGG-N-CCACG) is numbered once. All genes are sorted as in Online Table I, and all information is presented as in Online Table I.

Online Table III. Genes containing consensus UPRE elements within 2KB promoter regions. Each unique gene containing a consensus UPRE (TGACGTGGA) is numbered once. All genes are sorted as in Online Table I, and all information is presented as in Online Table I.

Online Table IV. Genes containing 1bp-mismatched ERSE elements within 2KB promoter regions.

Each unique gene containing an ERSE (CCAAT-N9-CCACG) with 1bp-mismatched anywhere on either flanking region, is numbered once. All ATF6-regulated genes are sorted by the fold change from our

previous array study.[2] The MGI symbol, alias or common name, and NCBI Reference Sequence ID, or accession number, is shown for each gene. More information about each gene can be obtained by entering the MGI symbol into the Mouse Genome Informatics (MGI 3.54) web site. Also shown is the Start and End location for each 1bp-mismatched ERSE identified, as determined by retrieving the 2000bp 5' flanking promoter sequence using Ensembl Biomart (http://www.ensembl.org/biomart/martview) and searching for each element with our custom Perl script.

Online Table V. Genes containing 1bp-mismatched ERSEII elements within 2KB promoter regions.

Each unique gene containing an ERSEII (ATTGG-N-CCACG) with 1bp-mismatched anywhere on either flanking region, is numbered once. All genes are sorted as in Online Table IV, and all information is presented as in Online Table IV.

Online Table VI. Genes containing 1bp-mismatched UPRE elements within 2KB promoter regions.

Each unique gene containing an UPRE (TGACGTGGA) with 1bp-mismatched anywhere on the element, is numbered once. All genes are sorted as in Online Table IV, and all information is presented as in Online Table IV.

Online Figure I. MI Increases 50KD ATF6 and Derl3 mRNA

Panels A-B: NTG mice were subjected to sham infarct surgery or to permanent occlusion myocardial infarction for the indicated times. Animals were then sacrificed and hearts were used to prepare tissue extracts for western blot analysis, as previously described (lanes 1-9).[10] To confirm the identity of the 50KD band, cell lysates from HeLa cells transfected with a 3xFlag-tagged ATF6 plasmid and subjected to the protease inhibitor ALLN (3mM) in order to preserve the labile, N-terminal form of ATF6, were loaded (lanes 10-11).

Panel C: NTG mice were subjected to sham infarct surgery or to permanent occlusion myocardial infarction for 1d, 4d, or 7d. Animals were then sacrificed and hearts were used to prepare tissue extracts for RT-qPCR, as previously described.[10] The numbers of animals used for each trial were as follows: sham n = 4; MI n= 7 to 8. * = $p \leq 0.05$ different from all other values determined by ANOVA.

Online Figure II. Derl3 Overexpression Attenuates ER Stress mRNA Activation Following sI and sI/R.

NRVMCs were infected $\pm$ AdVCon or AdV-Derl3 and 24h later, cultures were treated $\pm$ sI for 20h followed by sI/R for 24h **(Panels A and B)**, or $\pm$ sI for the indicated times **(Panels C and D)**. Cultures were then extracted and cell lysates were analyzed for the levels of the prototypical ERSR mRNAs, GRP78 and GRP94 (n = 3 cultures per treatment, sum of 2 separate experiments). Shown is the relative amount of each target mRNA/GAPDH, expressed as fold of AdVCon Con, $\pm$ S.E for each treatment. Panels A-B: *,+ = $p<0.05$ different from all other values by ANOVA, Panels C-D: * = $p<0.05$ from AdVCon Con by ANOVA.

The following primers were used:

GRP78: 5'-CACGTCCAACCCGGAGAA; 3' –ATTCCAAGTGCGTCCGATG

GRP94: 5' – TTGTGGATTCCGATGATCTCC; 3' – CAGAGTTTTGCGGACAAGCTT

GAPDH: 5' –CCTGGCCAAGGTCATCCAT; 3' – GTCATGAGCCCTTCCACGAT

References

1. Martindale JJ, Fernandez R, Thuerauf D, Whittaker R, Gude N, Sussman MA, Glembotski CC. Endoplasmic reticulum stress gene induction and protection from ischemia/reperfusion injury in the hearts of transgenic mice with a tamoxifen-regulated form of ATF6. *Circ Res*. 2006;98:1186-93.
2. Belmont PJ, Tadimalla A, Chen WJ, Martindale JJ, Thuerauf DJ, Marcinko M, Gude N, Sussman MA, Glembotski CC. Coordination of growth and endoplasmic reticulum stress signaling by regulator of calcineurin 1 (RCAN1), a novel ATF6-inducible gene. *J Biol Chem*. 2008;283:14012-21.
3. Aridor M. Visiting the ER: the endoplasmic reticulum as a target for therapeutics in traffic related diseases. *Adv Drug Deliv Rev*. 2007;59:759-81.
4. Kokame K, Kato H, Miyata T. Identification of ERSE-II, a new cis-acting element responsible for the ATF6-dependent mammalian unfolded protein response. *J Biol Chem*. 2001;276:9199-205.
5. Yoshida H, Haze K, Yanagi H, Yura T, Mori K. Identification of the cis-acting endoplasmic reticulum stress response element responsible for transcriptional induction of mammalian glucose-regulated proteins. Involvement of basic leucine zipper transcription factors. *J Biol Chem*. 1998;273:33741-9.
6. Efron B, Tibshirani R. Statistical Data Analysis in the Computer Age. *Science*. 1991;253:390-395.
7. Chen WH, Sun LT, Tsai CL, Song YL, Chang CF. Cold-stress induced the modulation of catecholamines, cortisol, immunoglobulin M, and leukocyte phagocytosis in tilapia. *Gen Comp Endocrinol*. 2002;126:90-100.
8. Thuerauf DJ, Marcinko M, Gude N, Rubio M, Sussman MA, Glembotski CC. Activation of the unfolded protein response in infarcted mouse heart and hypoxic cultured cardiac myocytes. *Circ Res*. 2006;99:275-82.
9. Doroudgar S, Thuerauf DJ, Marcinko MC, Belmont PJ, Glembotski CC. Ischemia activates the ATF6 branch of the endoplasmic reticulum (ER) stress response. *J Biol Chem*. 2009.
10. Tadimalla A, Belmont PJ, Thuerauf DJ, Glassy MS, Martindale JJ, Gude N, Sussman MA, Glembotski CC. Mesencephalic astrocyte-derived neurotrophic factor is an ischemia-inducible secreted endoplasmic reticulum stress response protein in the heart. *Circ Res*. 2008;103:1249-58.
11. Thuerauf DJ, Morrison L, Glembotski CC. Opposing roles for ATF6alpha and ATF6beta in endoplasmic reticulum stress response gene induction. *J Biol Chem*. 2004;279:21078-84.
12. Sifers RN, Brashears-Macatee S, Kidd VJ, Muensch H, Woo SL. A frameshift mutation results in a truncated alpha 1-antitrypsin that is retained within the rough endoplasmic reticulum. *J Biol Chem*. 1988;263:7330-5.
13. Hoover HE, Thuerauf DJ, Martindale JJ, Glembotski CC. alpha B-crystallin gene induction and phosphorylation by MKK6-activated p38. A potential role for alpha B-crystallin as a target of the p38 branch of the cardiac stress response. *J Biol Chem*. 2000;275:23825-33.

Online Table I.
Genes containing consensus ERSE elements within 2KB promoter regions

ATF6-Regulated Genes

Number	MGI symbol	Alias or Protein Name	NCBI RefSeq	Start	End	Strand	Fold Change
1	**Derlin-3**	**Degraded in ER protein 3**	**NM_024440**	**257**	**239**	**-**	**18.5**
1	**Derlin-3**	**Degraded in ER protein 3**	**NM_024440**	**155**	**137**	**-**	**18.5**
2	DNAJC3	P58; P58IPK	NM_008929	146	128	+	12.75
3	Hsp90b1	Tra1; GRP94	NM_011631	41	23	-	7.07
3	Hsp90b1	Tra1; GRP94	NM_011631	64	46	+	7.07
4	Calr	Calreticulin	NM_007591	161	143	-	5.29
5	Hspa5	GRP78	NM_022310	148	130	+	4.71
6	Syvn1	Synoviolin 1	NM_028769	129	111	+	4.6
7	XBP1	X-box binding protein 1	NM_013842	60	42	+	2.95

Full Genome

Number	MGI symbol	Alias or Protein Name	NCBI RefSeq	Start	End	Strand
1	Adamtsl5	ADAMTS-like 5	NM_001024139	591	573	-
2	Adcy3	adenylate cyclase 3	NM_027857	216	198	+
3	Alg12	asparagine-linked glycosylation 12 homolog	NM_145477	219	201	+
4	Calr	Calreticulin	NM_007591	161	143	-
5	Cd209d	CD209d antigen	NM_130904	666	648	+
6	Clec12a	C-type lectin domain family 12, member a	NM_177686	1919	1901	+
7	CNX	calnexin	NM_001110499	161	143	+
8	Creld2	cysteine-rich with EGF-like domains 2	NM_029720	125	107	-
9	Ddefl1	development and differentiation enhancing factor-like 1	NM_001008232	1504	1486	+
10	**Derlin-3**	**Degraded in ER protein 3**	NM_024440	**257**	**239**	**-**
10	**Derlin-3**	**Degraded in ER protein 3**	NM_024440	**155**	**137**	**-**
11	Dnajb14	DnaJ (Hsp40) homolog, subfamily B, member 14	XM_001473173	1784	1766	-
12	DNAJC3	P58; P58IPK	NM_008929	146	128	+
13	Ero1lb	ERO1-like beta	NM_026184	200	182	-
14	Foxk1	forkhead box K1	NM_010812	1227	1209	-
15	Grp45	G protein-coupled receptor 44	NM_009962	173	155	-
16	Hnrpa3	heterogeneous nuclear ribonucleoprotein A3	NM_053263	243	225	-
17	Hsp90b1	Tra1; GRP94	NM_011631	41	23	-
17	Hsp90b1	Tra1; GRP94	NM_011631	64	46	+
18	Hspa5	GRP78	NM_022310	64	46	+
19	Kbtbd8	kelch repeat and BTB (POZ) domain containing 8	NM_001008785	1165	1147	+
20	Kcna6	potassium voltage-gated channel, shaker-related, subfamily, member 6	NM_013568	1668	1650	+
21	Kcnmb2	potassium large conductance calcium-activated channel, subfamily M, beta member 2	NM_028231	1920	1902	-
22	Klk1b8	kallikrein 1-related peptidase b8	NM_008457	321	303	+
23	Klk1b22	kallikrein 1-related peptidase b22	NM_010114	318	300	+
24	Mfsd11	major facilitator superfamily domain containing 11	NM_178620	579	561	+
25	Nox3	NADPH oxidase 3	NM_198958	1045	1027	-
26	Nt5dc3	5'-nucleotidase domain containing 3	NM_175331	338	320	+
26	Nt5dc3	5'-nucleotidase domain containing 3	NM_175331	233	215	-
27	Pdia6	protein disulfide isomerase associated 6	NM_027959	103	85	+
28	Setbp1	SET binding protein 1	NM_053099	322	304	-
29	Sfrs2	splicing factor, arginine/serine-rich 2 (SC-35)	NM_011358	358	340	-
30	Syvn1	Synoviolin 1	NM_028769	129	111	+
31	Tmprss11e	transmembrane protease, serine 11e	NM_172880	1554	1536	+
32	Tmprss12	transmembrane protease, serine 12	NM_183109	1003	985	+
33	Usp52	ubiquitin specific peptidase 52	NM_133992	47	29	-
34	XBP1	X-box binding protein 1	NM_013842	60	42	+
35	Xlr3a	X-linked lymphocyte-regulated 3A	NM_001110784	171	153	+
36	Xlr3b	X-linked lymphocyte-regulated 3B	NM_001081643	148	130	+
37	Xlr3c	X-linked lymphocyte-regulated 3C	NM_011727	168	150	+
38	Zfp57	zinc finger protein 57	NM_001013745	49	31	-
39	Zfp777	zinc finger protein 777	NM_001081382	1948	1930	-

Online Table II.
Genes containing consensus ERSEII elements within 2KB promoter regions

ATF6-Regulated Genes

Number	MGI symbol	Alias or Protein Name	NCBI RefSeq	Start	End	Strand	Fold Change
1	Dnajb11	DnaJ (Hsp40) homolog, subfamily B, member 11	NM_026400	11	1	+	12.39
2	Armet	arginine-rich, mutated in early stage tumors	NM_029103	110	100	-	8.21
3	Hyou1	hypoxia up-regulated 1	NM_021395	178	168	-	3.864
3	Hyou1	hypoxia up-regulated 1	NM_021395	77	67	-	3.864
4	Herpud1	homocysteine-inducible, endoplasmic reticulum stress-inducible, ubiquitin-like domain member 1	NM_022331	117	107	+	2.43

Full Genome

Number	MGI symbol	Alias or Protein Name	NCBI RefSeq	Start	End	Strand
1	1110067D22Rik	Grpa	NM_173752	80	70	-
2	4933421E11Rik	Rif1	NM_001039478	67	57	+
3	1500005K14Rik	Fam101b	XM_893392	1067	1057	+
4	Apon	apolipoprotein N	NM_133996	1464	1454	-
5	Armet	arginine-rich, mutated in early stage tumors	NM_029103	110	100	-
6	Cxcl12	chemokine (C-X-C motif) ligand 12	NM_001012477	479	469	+
7	D430018E03Rik	RIKEN cDNA D430018E03 gene	NM_001002769	1449	1439	-
8	Dnajb11	DnaJ (Hsp40) homolog, subfamily B, member 11	NM_026400	11	1	+
9	Efhc1	EF-hand domain-containing protein 1	XM_129694	349	339	-
10	EG665305	LOC665305	XM_975981	123	113	-
11	Gal3st4	galactose-3-O-sulfotransferase 4	NM_001033416	865	855	+
12	Herpud1	homocysteine-inducible, endoplasmic reticulum stress-inducible, ubiquitin-like domain member 1	NM_022331	117	107	+
13	Hyou1	hypoxia up-regulated 1	NM_021395	178	168	-
13	Hyou1	hypoxia up-regulated 1	NM_021395	77	67	-
14	Iqcf5	IQ motif containing F5	XM_356185	740	730	-
15	Mcm9	minichromosome maintenance complex component 9	NM_027830	867	857	-
16	Ninj1	Ninjurin-1	NM_013610	781	771	+
17	Nrxn2	Neurexin II	XM_978630	100	90	-
18	Nucb1	nucleobindin 1	NM_008749	40	30	-
19	Rasd1	Dexras1	NM_009026	768	758	
20	Rbm39	RNA binding motif protein 39	NM_133242	80	70	+
21	Rcl1	RNA terminal phosphate cyclase-like 1	NM_021525	81	71	-
22	Rnf151	ring finger protein 151	NM_026205	33	23	+
23	Tbccd1	TBCC domain containing 1	NM_001081368	323	313	-
24	Tbx2	T-box 2	NM_009324	1913	1903	-
25	Tmed2	transmembrane emp24 domain trafficking protein 2	NM_019770	202	192	+
26	Tmem119	transmembrane protein 119	NM_146162	380	370	+
27	Trim46	tripartite motif-containing 46	NM_183037	1300	1290	-
28	Ufd1	ubiquitin fusion degradation 1 like	NM_011672	657	647	+
29	Ung	UDG	NM_001040691	1152	1142	-

Online Table III.
Genes containing consensus UPRE elements within 2KB promoter regions

ATF6-Regulated Genes

Number	MGI symbol	Alias or Protein Name	NCBI RefSeq	Start	End	Strand	Fold Change
1	Timp1	tissue inhibitor of metalloproteinase 1	NM_001044384	83	75	+	7.78
2	Stat3	signal transducer and activator of transcription 3	NM_011486	563	555	-	2.777
3	Fra-2	fos-like antigen 2	NM_008037	1118	1110	-	2.477
4	Nmor2	NAD(P)H dehydrogenase, quinone 2	NM_020282	539	531	+	0.3413
5	Kcnv2	potassium channel, subfamily V, member 2	NM_183179	124	116	-	0.179

Full Genome

Number	MGI symbol	Alias or Protein Name	NCBI RefSeq	Start	End	Strand
1	1110049F12Rik	RIKEN cDNA 1110049F12 gene	NM_025411	62	54	-
2	1810007P19Rik	RIKEN cDNA 1810007P19 gene	NM_172701	827	819	+
3	2010203O07Rik	DnaJ (Hsp40) homolog, subfamily C , member 25	NM_001033165	48	40	+
4	4921507L20Rik	RIKEN cDNA 4921507L20 gene	AK014837	1959	1951	+
5	4921530L21Rik	RIKEN cDNA 4921530L21 gene	NM_025733	1067	1059	+
6	4930579K19Rik	RIKEN cDNA 4930579K19 gene	NM_175227	138	130	+
7	9230112E08Rik	RIKEN cDNA 9230112E08 gene	NM_177264	197	189	+
8	9930038B18Rik	RIKEN cDNA 9930038B18 gene	NM_176929	1502	1494	-
9	Adam32	a disintegrin and metallopeptidase domain 32	NM_153397	1850	1842	+
10	Adamts17	a disintegrin-like and metallopeptidase (reprolysin type) with thrombospondin type 1 motif, 17	NM_001033877	660	652	-
11	Adrp	adipose differentiation related protein	NM_007408	1062	1054	+
12	Aff4	AF4/FMR2 family, member 4	NM_033565	470	462	-
13	Afg3l1	AFG3(ATPase family gene 3)-like 1 (yeast)	NM_054070	466	458	+
14	Alx3	aristaless-like homeobox 3	XM_973424	37	29	+
15	Aox3	aldehyde oxidase 3	NM_023617	228	220	-
16	Apbb1	amyloid beta (A4) precursor protein-binding, family B, member 1	NM_009685	778	770	-
17	Apc2	adenomatosis polyposis coli 2	NM_011789	1732	1724	-
18	Apobec3	apolipoprotein B editing complex 3	NM_030255	372	364	+
18	Apobec3	apolipoprotein B editing complex 3	NM_030255	1851	1843	+
19	App	amyloid beta (A4) precursor protein	NM_007471	638	630	-
20	Azi1	5-azacytidine induced gene 1	NM_001109658	698	690	-
21	B530045E10Rik	RIKEN cDNA B530045E10 gene	NM_177302	881	873	+
22	BC022687	cDNA sequence BC022687	NM_145450	1466	1458	+
23	BC031781	cDNA sequence BC031781	NM_145943	1503	1495	+
24	Brd9	bromodomain containing 9	NM_001024508	1813	1805	-
25	C130021I20Rik	Riken cDNA C130021I20 gene	NM_177842	110	102	-
26	C230094A16Rik	RIKEN cDNA C230094A16 gene	NM_146016	332	324	-
27	C330006K01Rik	RIKEN cDNA C330006K01 gene	NM_172725	186	178	+
28	Camta2	calmodulin binding transcription activator 2	NM_178116	1116	1108	+
29	Ccdc126	coiled-coil domain containing 126	NM_175098	1514	1506	+
30	CCS	copper chaperone for superoxide dismutase	NM_016892	1998	1990	+
31	Cd101	immunoglobulin superfamily, member 3	NM_207205	507	499	+
32	Cd3e	CD3 antigen, epsilon polypeptide	NM_007648	73	65	+
33	Cdk2ap1	CDK2 (cyclin-dependent kinase 2)-associated protein 1	NM_013812	1981	1973	+
34	Cenpp	centromere protein P	NM_025495	1690	1682	-
35	Chchd4	coiled-coil-helix-coiled-coil-helix domain containing 4	NM_133928	888	880	-
36	CHLFH1a	CKLF-like MARVEL transmembrane domain containing 1	NM_181990	599	591	-
37	Chrnb2	cholinergic receptor, nicotinic, beta polypeptide 2 (neuronal)	NM_009602	198	190	-
38	Clcn6	chloride channel 6	NM_011929	1740	1732	+
39	Clstn3	calsyntenin 3	NM_153508	367	359	+
40	Cmkbr6	chemokine (C-C motif) receptor 6	NM_009835	634	626	-
41	Col20a1	collagen, type XX, alpha 1	XM_001473208	664	656	-
42	Crtap	cartilage associated protein	NM_019922	1145	1137	+
43	Ctbs	chitobiase, di-N-acetyl-	NM_028836	1853	1845	+
44	Cul4a	cullin 4A	NM_146207	703	695	+
45	Cyb561	cytochrome b-561	NM_007805	236	228	+
46	Dchs1	dachsous 1	XM_993405	660	652	+
47	Dcun1d1	DCN1, defective in cullin neddylation 1, domain containing 1	NM_033623	320	312	+
48	Defb38	defensin beta 38	NM_183036	1399	1391	+
49	Dkk3	dickkopf homolog 3	NM_015814	1414	1406	-
50	Dscaml1	Down syndrome cell adhesion molecule-like 1	NM_001081270	787	779	-
51	Ebf4	early B-cell factor 4	NM_001110513	951	943	+
52	EG245174	predicted gene, EG245174	XM_001480860	403	395	-
53	Eif2a	eukaryotic translation initiation factor 2a	NM_001005509	823	815	-
54	Fank1	fibronectin type 3 and ankyrin repeat domains 1	NM_025850	71	63	-
55	Fbxo9	f-box protein 9	NM_001081490	188	180	+
56	Fer1l4	fer-1-like 4	XM_001481335	417	409	+
57	Fgfbp1	fibroblast growth factor binding protein 1	NM_008009	1931	1923	-
58	Fpgt	fucose-1-phosphate guanylyltransferase	NM_029330	69	61	+
59	Fra-2	fos-like antigen 2	NM_008037	1118	1110	-
60	Fscn3	fascin homolog 3, actin-bundling protein, testicular (Strongylocentrotus purpuratus)	NM_019569	1230	1222	+
61	Gabarap	gamma-aminobutyric acid receptor associated protein	NM_019749	464	456	+
62	Gabpb1	GA repeat binding protein, beta 1	NM_207669	568	560	-
63	Gcg	glucagon	NM_008100	1175	1167	+
64	Gfra1	glial cell line derived neurotrophic factor family receptor alpha 1	NM_010279	696	688	+
65	Glut4	solute carrier family 2 (facilitated glucose transporter), member 4	NM_009204	1890	1882	-
66	Gnai3	guanine nucleotide binding protein (G protein), alpha inhibiting 3	NM_010306	1028	1020	+

Online Table III.
Genes containing consensus UPRE elements within 2KB promoter regions

Full Genome (Continued)

Number	MGI symbol	Alias or Protein Name	NCBI RefSeq	Start	End	Strand
67	Gosr2	golgi SNAP receptor complex member 2	NM_019650	471	463	-
68	Gria3	glutamate receptor, ionotropic, AMPA3 (alpha 3)	NM_016886	668	660	-
69	Gtf2h2	general transcription factor II H, polypeptide 2	NM_022011	805	797	-
70	Gtf2h4	general transcription factor II H, polypeptide 4	NM_010364	632	624	-
71	H1fx	H1 histone family, member X	XM_981507	1795	1787	-
72	Hbs1l	Hbs1-like (S. cerevisiae)	NM_001042593	122	114	-
73	Hk2	hexokinase 2	XM_00147807	48	40	-
74	Hoxa11	homeo box A11	NM_010450	20	12	-
75	Igf2r	insulin-like growth factor 2 receptor	NM_010515	1719	1711	-
76	IL-10	interleukin 10	NM_010548	355	347	-
77	Isg20	interferon-stimulated protein	NM_001113527	95	87	-
78	Kbtbd11	kelch repeat and BTB (POZ) domain containing 11	XM_921147	710	702	+
79	Kcnk6	potassium inwardly-rectifying channel, subfamily K, member 6	NM_001033525	1305	1297	-
80	Kcnv2	potassium channel, subfamily V, member 2	NM_183179	124	116	-
81	Lcat	lecithin cholesterol acyltransferase	NM_008490	1211	1203	+
82	Lmx1b	LIM homeobox transcription factor 1 beta	NM_010725	619	611	+
83	Lrrc58	leucine rich repeat containing 58	XM_915566	793	785	+
84	Maoa	monoamine oxidase A	NM_173740	1228	1220	+
85	Menkes	ATPase, Cu++ transporting, alpha polypeptide	NM_001109757	175	167	+
86	Mga	MAX gene associated	NM_013720	9	1	+
87	MGBmper	BMP-binding endothelial regulator	NM_028472	1178	1170	-
88	Mpzl3	myelin protein zero-like 3	NM_001093749	560	552	-
89	Mthfr	5,10-methylenetetrahydrofolate reductase	NM_010840	644	636	-
90	Mycbpap	Mycbp associated protein	NM_170671	496	488	+
91	Ncstn	nicastrin	NM_021607	92	84	-
92	Necab2	N-terminal EF-hand calcium binding protein 2	XM_001001292	966	958	+
93	Neurl2	Neurl2	NM_001081656	1675	1667	+
94	Nfe2l1	nuclear factor, erythroid derived 2,-like 1	NM_001130453	171	163	-
95	Nmor2	NAD(P)H dehydrogenase, quinone 2	NM_020282	572	564	+
96	Nod1	nucleotide-binding oligomerization domain containing 1	NM_172729	1495	1487	-
97	Olfr837	olfactory receptor 837	NM_146565	1960	1952	+
98	Ormdl3	ORM1-like 3	NM_025661	980	972	+
99	Paqr9	progestin and adipoQ receptor family member IX	NM_198414	740	732	+
100	Park7	Parkinson disease (autosomal recessive, early onset)	NM_020569	413	405	+
101	Pax-1	paired box gene 1	NM_008780	48	40	+
102	Pdgfd	platelet-derived growth factor, D polypeptide	NM_027924	65	57	-
103	Rbks	ribokinase	NM_153196	866	858	-
104	Rlbp1l1	retinaldehyde binding protein 1-like 1	NM_028940	809	801	+
105	Rnf213	ring finger protein 213	NM_001040005	1754	1746	+
106	Serpini1	serine (or cysteine) peptidase inhibitor, clade I, member 1	NM_009250	1609	1601	-
107	Sez6l2	seizure related 6 homolog like 2	NM_144926	1974	1966	-
108	Sgk2	serum/glucocorticoid regulated kinase 2	XM_984112	1712	1704	+
109	Sgk3	serum/glucocorticoid regulated kinase 3	NM_177547	619	611	+
110	Slc16a8	solute carrier family 16 (monocarboxylic acid transporters), member 8	NM_020516	1740	1732	-
111	Slc19a3	solute carrier family 19 (sodium/hydrogen exchanger), member 3	NM_030556	189	181	+
112	Sncaip	synuclein, alpha interacting protein (synphilin)	NM_026408	1118	1110	-
113	Sohlh2	spermatogenesis and oogenesis specific basic helix-loop-helix 2	NM_028937	87	79	-
114	Sp4	trans-acting transcription factor 4	NM_009239	1571	1563	-
115	Stat3	signal transducer and activator of transcription 3	NM_011486	563	555	-
116	Ston1	stonin 1	NM_029858	589	581	+
117	Tas1r1	taste receptor, type 1, member 1	NM_031867	1538	1530	-
118	Thnsl1	threonine synthase-like 1	NM_177588	1665	1657	-
119	Timp1	tissue inhibitor of metalloproteinase 1	NM_001044384	83	75	+
120	Tmem102	transmembrane protein 102	NM_001033433	1389	1381	-
121	Tmem104	transmembrane protein 104	NM_001033393	360	352	-
122	Tpbpa	trophoblast specific protein alpha	NM_009411	338	330	-
123	Trcg1	taste receptor protein 1	NM_001014398	1899	1891	+
124	Trim8	tripartite motif protein 8	NM_053100	208	200	-
125	Tsc22d3	TSC22 domain family, member 3	NM_001077364	1897	1889	+
126	Tsfm	Ts translation elongation factor, mitochondrial	NM_025537	1054	1046	-
127	Ttc27	tetratricopeptide repeat domain 27	NM_152817	901	893	-
128	Txdc11	thioredoxin domain containing 11	NM_029582	60	52	+
129	Ubqln3	ubiquilin 3	NM_198623	1073	1065	+
129	Ubqln3	ubiquilin 3	NM_198623	1919	1911	-
130	Wfikkn2	WAP, follistatin/kazal, immunoglobulin, kunitz and netrin domain containing 2	NM_181819	561	553	-
131	Zfhx3	zinc finger homeobox 3	NM_007496	265	257	+
132	Zfp653	zinc finger protein 653	NM_177318	1649	1641	+

Online Table IV.
Genes containing 1bp-mismatched ERSE elements within 2KB promoter regions

ATF6-Regulated Genes

Number	MGI symbol	Alias or Protein Name	NCBI RefSeq	Start	End	Strand	Fold Change
1	Alkbh2	alkB, alkylation repair homolog 2	NM_175016	534	516	+	47.45
2	Il-6	interleukin 6	NM_031168	134	116	+	38.45
3	Pdia4	protein disulfide isomerase associated 4	NM_009787	107	89	-	16.37
4	Ears2	glutamyl-tRNA synthetase 2 (mitochondrial)(putative)	NM_026140	91	73	-	7.841
5	Eda2r	ectodysplasin A2 isoform receptor	NM_175540	1590	1572	+	7.464
6	Hsp90b1	heat shock protein 90, beta (Grp94), member 1	NM_011631	1287	1269	-	7.071
6	Hsp90b1	heat shock protein 90, beta (Grp94), member 1	NM_011631	185	167	-	7.071
7	Kpnb1	karyopherin (importin) beta 1	NM_008379	1328	1310	+	6.42
8	Sel1h	sel-1 suppressor of lin-12-like	NM_001039089	190	172	+	6.297
9	Tubb3	tubulin, beta 3	NM_023279	777	759	+	5.795
10	Edem1	ER degradation enhancer, mannosidase alpha-like 1	NM_138677	299	281	-	5.36
11	G530011O06Rik	RIKEN cDNA G530011O06 gene	NM_001039559	595	577	+	5.216
12	Trim37	tripartite motif-containing 37	NM_197987	239	221	-	5.208
12	Trim37	tripartite motif-containing 37	NM_197987	228	210	+	5.208
13	Kcnq1	potassium voltage-gated channel, subfamily Q, member 1	NM_008434	1891	1873	+	5.136
14	Ubfd1	ubiquitin family domain containing 1	NM_138589	79	61	+	5.048
15	Pdia3	protein disulfide isomerase associated 3	NM_007952	28	10	+	4.718
16	Arntl	aryl hydrocarbon receptor nuclear translocator-like	NM_007489	291	273	+	4.267
17	Tbcb	tubulin folding cofactor B	NM_025548	35	17	-	4.188
18	Pin1	protein (peptidyl-prolyl cis/trans isomerase) NIMA-interacting 1	NM_023371	100	82	-	4.119
19	2610036L11Rik	RIKEN cDNA 2610036L11 gene	NM_001109747	47	29	+	4.106
20	Hyou1	hypoxia up-regulated 1	NM_021395	513	495	+	3.864
21	p97/VCP	valosin containing protein	NM_009503	263	245	+	3.288
22	Rabepk	Rab9 effector protein with kelch motifs	NM_145522	168	150	-	3.066
23	Ptpn14	protein tyrosine phosphatase, non-receptor type 14	NM_001033287	1377	1359	+	3.045
24	Gsk3b	glycogen synthase kinase 3 beta	NM_019827	217	199	+	2.998
24	Gsk3b	glycogen synthase kinase 3 beta	NM_019827	1441	1423	-	2.998
25	Sfpq	splicing factor proline/glutamine rich (polypyrimidine tract binding protein associated)	XM_994784	1725	1707	-	2.906
26	Nmt1	N-myristoyltransferase 1	NM_008707	29	11	+	2.832
27	Fkbp11	FK506 binding protein 11	NM_024169	1089	1071	+	2.814
28	Ormdl2	ORM1-like 2	NM_024180	1673	1655	-	2.785
29	Tmem45a	transmembrane protein 45a	NM_019631	961	943	+	2.756
30	Rasl11b	RAS-like, family 11, member B	NM_026878	760	742	-	2.54
30	Rasl11b	RAS-like, family 11, member B	NM_026878	87	69	-	2.54
31	Nip7	nuclear import 7 homolog	NM_025391	32	14	-	2.513
32	Herpud1	homocysteine-inducible, endoplasmic reticulum stress-inducible, ubiquitin-like domain member 1	NM_022331	83	65	+	2.4315
33	Ngdn	neuroguidin, EIF4E binding protein	NM_026890	1844	1826	+	2.379
34	Mrps18b	mitochondrial ribosomal protein S18B	NM_025878	499	481	-	2.228
35	Lip1	lysosomal acid lipase A	NM_001111100	91	73	-	2.21
36	Ddx54	DEAD (Asp-Glu-Ala-Asp) box polypeptide 54	NM_028041	1142	1124	+	2.189
36	Ddx54	DEAD (Asp-Glu-Ala-Asp) box polypeptide 54	NM_028041	1204	1186	+	2.189
37	Stmn1	stathmin 1	NM_019641	1034	1016	-	2.143
38	Dnaja4	DnaJ (Hsp40) homolog, subfamily A, member 4	NM_021422	1834	1816	+	2.107
38	Dnaja4	DnaJ (Hsp40) homolog, subfamily A, member 4	NM_021422	350	332	+	2.107
39	Tubb5	tubulin, beta 5	NM_011655	158	140	+	2.084
40	Popdc3	popeye domain containing 3	NM_024286	1592	1574	+	2.043
41	Crls1	cardiolipin synthase 1	NM_025646	662	644	-	2.037
42	Enpp5	ectonucleotide pyrophosphatase/phosphodiesterase 5	NM_032003	741	723	-	0.495
43	Jam2	junction adhesion molecule 2	NM_023844	470	452	+	0.487
44	Auh	AU RNA binding protein/enoyl-coenzyme A hydratase	NM_016709	1410	1392	+	0.475
45	Ppil1	Cypl1	NM_025646	913	895	-	0.47
46	B3gnt6	UDP-GlcNAc:betaGal beta-1,3-N-acetylglucosaminyltransferase 6 (core 3 synthase)	NM_001081167	1138	1120	+	0.46
47	2410012H22Rik	zinc finger, SWIM-type containing 7	XM_001473892	575	557	+	0.45
48	Egflam	EGF-like, fibronectin type III and laminin G domains	NM_178748	189	171	+	0.435
49	Hrasls	HRAS-like suppressor	NM_013751	141	123	-	0.428
50	Myh6	myosin, heavy polypeptide 6, cardiac muscle, alpha	NM_010856	773	755	-	0.398
51	Cog8	component of oligomeric golgi complex 8	NM_139229	188	170	+	0.384
52	Siae	sialic acid acetylesterase	NM_011734	1525	1507	+	0.365
53	Nit2	nitrilase family, member 2	NM_023175	1041	1023	+	0.36
54	Asb14	ankyrin repeat and SOCS box-containing 14	NM_080856	1045	1027	+	0.187
55	Fbp2	fructose bisphosphatase 2	NM_007994	1068	1050	+	0.159
56	Acsm5	acyl-CoA synthetase medium-chain family member 5	NM_178758	287	269	-	0.0961
57	Ogdh	oxoglutarate dehydrogenase (lipoamide)	NM_010956	133	115	+	0.0828
58	Apba3	amyloid beta (A4) precursor protein binding, family A, member 1	NM_177034	600	582	-	0.0753

Online Table V.
Genes containing 1bp-mismatched ERSEII elements within 2KB promoter regions

ATF6-Regulated Genes

Number	MGI symbol	Alias or Protein Name	NCBI RefSeq	Start	End	Strand	Fold Change
1	Sdf2l1	stromal cell-derived factor 2-like 1	NM_022324	166	156	-	17.41
2	Tspyl2	TSPY-like 2	NM_029836	1326	1316	+	9.294
3	Ears2	glutamyl-tRNA synthetase 2 (mitochondrial)(putative)	NM_026140	351	341	+	7.841
4	Sel1h	sel-1 suppressor of lin-12-like	NM_001039089	161	151	-	6.297
5	D16Ertd472e	DNA segment, Chr 16, ERATO Doi 472, expressed	NM_025967	315	305	-	6.255
6	Edem1	ER degradation enhancer, mannosidase alpha-like 1	NM_138677	201	191	-	5.36
7	Ebp	phenylalkylamine Ca2+ antagonist (emopamil) binding protein	NM_007898	460	450	+	5.287
8	Atf4	activating transcription factor 4	NM_009716	81	71	-	4.928
9	Hspa5	heat shock protein 5, GRP78	NM_022310	103	93	-	4.706
10	Syvn1	synovial apoptosis inhibitor 1, synoviolin	NM_028769	154	144	+	4.5995
11	Arntl	aryl hydrocarbon receptor nuclear translocator-like	NM_007489	288	278	+	4.267
12	Egr-1	early growth response 1	NM_007913	342	332	-	3.667
13	Junb	Jun-B oncogene	NM_008416	360	350	-	2.639
14	Fra-2	fos-like antigen 2	NM_008037	1051	1041	-	2.477
15	3110050N22Rik	RIKEN cDNA 3110050N22 gene	NM_173181	23	13	-	2.396
16	Stt3b	STT3, subunit of the oligosaccharyltransferase complex, homolog B	NM_024222	191	181	+	2.228
17	Rpl14	ribosomal protein L14	NM_025974	80	70	-	2.087
18	Pank1	pantothenate kinase 1	NM_001114339	81	71	-	0.401
19	Slc22a5	solute carrier family 22 (organic cation transporter), member 5	NM_011396	246	236	-	0.3895
20	Acot11	acyl-CoA thioesterase 11	NM_025590	160	150	+	0.34
21	Tfdp2	transcription factor Dp 2	XM_001481271	110	100	-	0.335
22	Tfdp2	transcription factor Dp 2	XM_001481271	557	547	+	0.335
23	Asb10	ankyrin repeat and SOCS box-containing 10	NM_080444	516	506	-	0.231
24	ACH2	acyl-CoA thioesterase 1	NM_012006	1238	1228	-	0.225
25	Acot1	acyl-CoA thioesterase 1	NM_012006	686	676	-	0.225

Online Table VI.
Genes containing 1bp-mismatched UPRE elements within 2KB promoter regions

ATF6-Regulated Genes

Number	MGI symbol	Alias or Protein Name	NCBI RefSeq	Start	End	Strand	Fold Change
1	Far1	fatty acyl CoA reductase 1	NM_027379	131	123	+	120.9
2	Spp1	secreted phosphoprotein 1	NM_009263	1645	1637	+	91.47
3	Il-6	interleukin 6	NM_031168	886	878	+	38.45
4	Tk-1	thymidine kinase 1	NM_009387	745	737	+	20.57
5	Sdf2l1	stromal cell-derived factor 2-like 1	NM_022324	1539	1531	-	17.41
5	Sdf2l1	stromal cell-derived factor 2-like 1	NM_022324	1456	1448	-	17.41
6	Pdia4	protein disulfide isomerase associated 4	NM_009787	838	830	-	16.37
7	Dnajc3	DnaJ (Hsp40) homolog, subfamily C, member 3	NM_008929	194	186	-	12.75
8	Pgp	phosphoglycolate phosphatase	NM_025954	1099	1091	-	10.09
8	Pgp	phosphoglycolate phosphatase	NM_025954	386	378	+	10.09
9	eIF-1A	eukaryotic translation initiation factor 1A	NM_010120	81	73	+	9.657
10	P4hb	prolyl 4-hydroxylase, beta polypeptide	NM_011032	924	916	-	9.173
11	Chac1	ChaC, cation transport regulator-like 1	NM_026929	1603	1595	-	8.065
11	Chac1	ChaC, cation transport regulator-like 1	NM_026929	979	971	-	8.065
12	Hsp90b1	heat shock protein 90, beta (Grp94), member 1	NM_011631	823	815	+	7.071
12	Hsp90b1	heat shock protein 90, beta (Grp94), member 1	NM_011631	665	657	+	7.071
13	Itgam	integrin alpha M	NM_001082960	590	582	+	6.878
14	Hn1l	hematological and neurological expressed 1-like	NM_198937	1061	1053	+	6.772
15	Dbf4	DBF4 homolog	NM_013726	1383	1375	-	6.442
16	Sel1h	sel-1 suppressor of lin-12-like	NM_001039089	1652	1644	-	6.297
17	D16Ertd472e	DNA segment, Chr 16, ERATO Doi 472, expressed	NM_025967	1986	1978	+	6.255
18	2810474O19Rik	RIKEN cDNA 2810474O19 gene	NM_026054	1509	1501	+	6.0485
19	M(beta)2	tubulin, beta 2a	NM_009450	1604	1596	+	5.579
19	M(beta)2	tubulin, beta 2a	NM_009450	1222	1214	-	5.579
20	Tubb2b	tubulin, beta 2b	NM_023716	1957	1949	-	5.579
21	Fem1b	feminization 1 homolog b	NM_010193	881	873	+	5.325
22	Morf4l2	mortality factor 4 like 2	NM_019768	902	894	-	5.32
22	Morf4l2	mortality factor 4 like 2	NM_019768	1105	1097	+	5.32
23	G530011O06Rik	RIKEN cDNA G530011O06 gene	NM_001039559	1815	1807	-	5.216
24	Kcna9	potassium voltage-gated channel, subfamily Q, member 1	NM_008434	1928	1920	-	5.136
25	TSA903	uridine-cytidine kinase 2	NM_030724	423	415	+	5.0273
26	Rbm15b	RNA binding motif protein 15B	NM_175402	1302	1294	-	4.989
27	Rras2	related RAS viral (r-ras) oncogene homolog 2	NM_025846	1075	1067	-	4.947
27	Rras2	related RAS viral (r-ras) oncogene homolog 2	NM_025846	224	216	-	4.947
28	Aldh18a1	aldehyde dehydrogenase 18 family, member A1	NM_019698	1768	1760	+	4.8045
29	Grp58	protein disulfide isomerase associated 3	NM_007952	484	476	+	4.718
30	Ms4a4c	membrane-spanning 4-domains, subfamily A, member 4C	NM_029499	694	686	+	4.565
31	Plac8	placenta-specific 8	NM_139198	721	713	-	4.559
31	Plac8	placenta-specific 8	NM_139198	1433	1425	+	4.559
32	Kif5b	kinesin family member 5B	NM_008448	119	111	+	4.55
33	Nans	N-acetylneuraminic acid synthase (sialic acid synthase)	NM_053179	42	34	+	4.5345
34	Nola2	nucleolar protein family A, member 2	NM_026631	1215	1207	-	4.441
35	Map3k3	mitogen-activated protein kinase kinase kinase 3	NM_011947	13	5	+	4.287
36	Bmal1	aryl hydrocarbon receptor nuclear translocator-like	NM_007489	1388	1380	-	4.267
37	Tbcb	tubulin folding cofactor B	NM_025548	1014	1006	+	4.188
38	2610036L11Rik	RIKEN cDNA 2610036L11 gene	NM_001109747	1175	1167	+	4.106
39	Hmgb1	high mobility group box 1	NM_010439	962	970	+	4.083
40	Hagh	hydroxyacyl glutathione hydrolase	NM_024284	1761	1753	+	3.1413
40	Hagh	hydroxyacyl glutathione hydrolase	NM_024284	1504	1496	+	3.1413
40	Hagh	hydroxyacyl glutathione hydrolase	NM_024284	794	786	-	3.1413
41	Mesdc2	mesoderm development candidate 2	NM_023403	306	298	+	3.139
42	Serpinh1	serine (or cysteine) peptidase inhibitor, clade H, member 1	NM_001111044	315	307	-	3.097
43	Gsk3b	glycogen synthase kinase 3 beta	NM_019827	1288	1280	-	2.998
44	2700049P18Rik	RIKEN cDNA 2700049P18 gene	NM_175382	570	562	+	2.984
45	Flnc	filamin C, gamma (actin binding protein 280)	NM_001081185	1973	1965	-	2.9105
46	Dlgap4	discs, large homolog-associated protein 4	NM_001042488	407	399	+	2.907
46	Dlgap4	discs, large homolog-associated protein 4	NM_001042488	1591	1583	-	2.907
47	Nol12	nucleolar protein 12	NM_133800	1268	1260	+	2.888
48	Mettl1	methyltransferase-like 1	NM_010792	1029	1021	-	2.873
49	Srm	spermidine synthase	NM_009272	905	897	-	2.812
50	H2-Ke6	H2-K region expressed gene 6	NM_013543	934	926	+	2.719
51	Os9	amplified in osteosarcoma	NM_177614	1935	1927	-	2.672
52	Med19	mediator of RNA polymerase II transcription, subunit 19 homolog	NM_025885	989	981	-	2.66
53	Apex1	apurinic/apyrimidinic endonuclease 1	NM_009687	569	561	-	2.632

Online Table VI.
Genes containing 1bp-mismatched UPRE elements within 2KB promoter regions

Full Genome (Continued)

Number	MGI symbol	Alias or Protein Name	NCBI RefSeq	Start	End	Strand	Fold Change
54	Cyb5r1	cytochrome b5 reductase 1	NM_028057	220	212	-	2.597
55	Pja2	praja 2, RING-H2 motif containing	NM_001025309	968	960	+	2.568
55	Pja2	praja 2, RING-H2 motif containing	NM_001025309	706	698	+	2.568
55	Pja2	praja 2, RING-H2 motif containing	NM_001025309	676	668	+	2.568
55	Pja2	praja 2, RING-H2 motif containing	NM_001025309	646	638	+	2.568
55	Pja2	praja 2, RING-H2 motif containing	NM_001025309	616	608	+	2.568
55	Pja2	praja 2, RING-H2 motif containing	NM_001025309	586	578	+	2.568
55	Pja2	praja 2, RING-H2 motif containing	NM_001025309	556	548	+	2.568
55	Pja2	praja 2, RING-H2 motif containing	NM_001025309	526	518	+	2.568
55	Pja2	praja 2, RING-H2 motif containing	NM_001025309	496	488	+	2.568
55	Pja2	praja 2, RING-H2 motif containing	NM_001025309	466	458	+	2.568
55	Pja2	praja 2, RING-H2 motif containing	NM_001025309	436	428	+	2.568
55	Pja2	praja 2, RING-H2 motif containing	NM_001025309	939	931	+	2.568
55	Pja2	praja 2, RING-H2 motif containing	NM_001025309	406	398	+	2.568
55	Pja2	praja 2, RING-H2 motif containing	NM_001025309	376	368	+	2.568
55	Pja2	praja 2, RING-H2 motif containing	NM_001025309	346	338	+	2.568
55	Pja2	praja 2, RING-H2 motif containing	NM_001025309	316	308	+	2.568
55	Pja2	praja 2, RING-H2 motif containing	NM_001025309	286	278	+	2.568
55	Pja2	praja 2, RING-H2 motif containing	NM_001025309	256	248	+	2.568
55	Pja2	praja 2, RING-H2 motif containing	NM_001025309	226	218	+	2.568
55	Pja2	praja 2, RING-H2 motif containing	NM_001025309	196	188	+	2.568
55	Pja2	praja 2, RING-H2 motif containing	NM_001025309	910	902	+	2.568
55	Pja2	praja 2, RING-H2 motif containing	NM_001025309	881	873	+	2.568
55	Pja2	praja 2, RING-H2 motif containing	NM_001025309	852	844	+	2.568
55	Pja2	praja 2, RING-H2 motif containing	NM_001025309	823	815	+	2.568
55	Pja2	praja 2, RING-H2 motif containing	NM_001025309	794	786	+	2.568
55	Pja2	praja 2, RING-H2 motif containing	NM_001025309	765	757	+	2.568
55	Pja2	praja 2, RING-H2 motif containing	NM_001025309	736	728	+	2.568
56	Sec11a	SEC11 homolog A	NM_019951	1759	1751	-	2.528
57	Trove2	TROVE domain family, member 2	NM_013835	236	228	-	2.5145
58	Nip7	nuclear import 7 homolog	NM_025391	561	553	-	2.513
59	Heatr5a	HEAT repeat containing 5A	NM_177171	1031	1023	+	2.512
60	Rap2b	RAP2B, member of RAS oncogene family	NM_028712	1437	1429	+	2.454
61	Ywhaz	tyrosine 3-monooxygenase/tryptophan 5-monooxygenase activation protein, zeta polypeptide	NM_011740	92	84	-	2.446
62	Gmppb	GDP-mannose pyrophosphorylase B	NM_177910	1739	1731	-	2.437
63	Ehd4	EH-domain containing 4	NM_133838	353	345	-	2.403
64	3110050N22Rik	RIKEN cDNA 3110050N22 gene	NM_173181	191	183	+	2.396
65	Ngd	neuroguidin, EIF4E binding protein	NM_026890	1576	1568	-	2.379
65	Ngd	neuroguidin, EIF4E binding protein	NM_026890	743	735	+	2.379
66	LOC217431	nucleolar protein 10	NM_001008421	282	274	+	2.373
67	Ing1	inhibitor of growth family, member 1	XM_976943	518	510	+	2.369
67	Ing1	inhibitor of growth family, member 1	XM_976943	1333	1325	+	2.369
68	Cldnd1	claudin domain containing 1	NM_171826	809	801	-	2.338
69	Pdap1	PDGFA associated protein 1	NM_001033313	931	923	+	2.336
70	Nucks1	nuclear casein kinase and cyclin-dependent kinase substrate 1	NM_175294	1921	1913	+	2.326
70	Nucks1	nuclear casein kinase and cyclin-dependent kinase substrate 1	NM_175294	274	266	+	2.326
71	Gcs1	glucosidase 1	NM_020619	33	25	+	2.323
72	1700025G04Rik	RIKEN cDNA 1700025G04 gene	NM_197990	1978	1970	-	2.2625
73	Pde4b	phosphodiesterase 4B, cAMP specific	NM_019840	253	245	-	2.216
73	Pde4b	phosphodiesterase 4B, cAMP specific	NM_019840	1062	1054	-	2.216
74	Fads3	fatty acid desaturase 3	NM_021890	1516	1508	-	2.21
75	Slc6a6	solute carrier family 6 (neurotransmitter transporter, taurine), member 6	NM_009320	1768	1760	+	2.207
75	Slc6a6	solute carrier family 6 (neurotransmitter transporter, taurine), member 6	NM_009320	480	472	-	2.207
76	Adamts15	a disintegrin-like and metallopeptidase (reprolysin type) with thrombospondin type 1 motif, 15	NM_001024139	52	44	-	2.182
77	Tln1	talin 1	NM_011602	1444	1436	+	2.137
77	Tln1	talin 1	NM_011602	1060	1052	+	2.137

Online Table VI.
Genes containing 1bp-mismatched UPRE elements within 2KB promoter regions

Full Genome (Continued)

Number	MGI symbol	Alias or Protein Name	NCBI RefSeq	Start	End	Strand	Fold Change
78	Tmem57	transmembrane protein 57	NM_025382	735	727	+	2.136
79	Rrbp1	ribosome binding protein 1	NM_024281	626	618	-	2.114
80	Rrbp1	ribosome binding protein 1	NM_024281	311	303	+	2.114
81	Ralb	v-ral simian leukemia viral oncogene homolog B (ras related)	NM_022327	1719	1711	+	2.109
82	tTGas	transglutaminase 2, C polypeptide	NM_009373	1498	1490	-	2.106
83	Srxn1	sulfiredoxin 1 homolog	NM_029688	750	742	+	2.084
84	Stip1	stress-induced phosphoprotein 1	NM_016737	1476	1468	+	2.051
85	Rps27l	ribosomal protein S27-like	NM_026467	1848	1840	-	2.05
86	Crls1	cardiolipin synthase 1	NM_025646	1192	1184	+	2.037
87	B3galtl	beta 1,3-galactosyltransferase-like	NM_194318	586	578	-	0.494
88	Rhobtb1	Rho-related BTB domain containing 1	NM_001081347	624	616	-	0.478
89	Lmod2	leiomodin 2 (cardiac)	NM_053098	615	607	+	0.473
90	Clip4	CAP-GLY domain containing linker protein family, member 4	NM_175378	1672	1664	-	0.472
91	3110002H16Rik	RIKEN cDNA 3110002H16 gene	NM_029623	1093	1085	+	0.461
91	3110002H16Rik	RIKEN cDNA 3110002H16 gene	NM_029623	23	15	+	0.461
92	Lpl	lipoprotein lipase	NM_008509	1987	1979	+	0.459
93	Cbr1	carbonyl reductase 1	NM_007620	1061	1053	+	0.451
94	Ccni	cyclin I	NM_017367	519	511	-	0.445
95	Grb14	growth factor receptor bound protein 14	NM_016719	1187	1179	+	0.44
96	Neo1	neogenin	NM_001042752	1193	1185	-	0.427
97	Atp6v0e2	ATPase, H+ transporting, lysosomal V0 subunit E2	NM_133764	1191	1183	+	0.42
97	Atp6v0e2	ATPase, H+ transporting, lysosomal V0 subunit E2	NM_133764	542	534	+	0.42
98	Sirt5	sirtuin 5 (silent mating type information regulation 2 homolog) 5	NM_178848	20	12	+	0.403
98	Sirt5	sirtuin 5 (silent mating type information regulation 2 homolog)	NM_178848	1344	1336	-	0.403
99	Gramd1b	GRAM domain containing 1B	NM_172768	1577	1569	+	0.396
100	Mrpl49	mitochondrial ribosomal protein L49	NM_026246	1216	1208	-	0.395
100	Mrpl49	mitochondrial ribosomal protein L49	NM_026246	1230	1222	-	0.395
101	Asb11	ankyrin repeat and SOCS box-containing 11	NM_026853	90	82	-	0.383
102	Mfsd4	major facilitator superfamily domain containing 4	NM_001114662	973	965	-	0.361
102	Mfsd4	major facilitator superfamily domain containing 4	NM_001114662	235	227	+	0.361
103	D930001I22Rik	RIKEN cDNA D930001I22 gene	NM_173397	427	419	-	0.357
104	Ak3	adenylate kinase 3	NM_021299	454	446	-	0.3505
105	Gdc1	glycerol-3-phosphate dehydrogenase 1 (soluble)	NM_010271	1384	1376	+	0.342
106	Retsat	retinol saturase (all trans retinol 13,14 reductase)	NM_026159	1863	1855	-	0.34
106	Ccdc69	coiled-coil domain containing 69	NM_177471	82	74	+	0.331
107	gamma-SG	sarcoglycan, gamma (dystrophin-associated glycoprotein)	NM_011892	1227	1219	+	0.317
108	Gpcr10	endothelin receptor type A	NM_010332	1954	1946	-	0.3167
109	Cutc	cutC copper transporter homolog	NM_001113562	128	120	-	0.307
110	ORF28	DnaJ (Hsp40) homolog, subfamily C, member 28	NM_001099738	1820	1812	+	0.302
111	Sord	sorbitol dehydrogenase	NM_146126	218	210	-	0.295
112	Ucp3	uncoupling protein 3 (mitochondrial, proton carrier)	NM_009464	1723	1715	-	0.27
112	Ucp3	uncoupling protein 3 (mitochondrial, proton carrier)	NM_009464	925	917	-	0.27
113	Asb2	ankyrin repeat and SOCS box-containing 2	XM_977692	51	43	-	0.249
114	Fndc5	fibronectin type III domain containing 5	NM_027402	166	158	+	0.243
115	Acy3	aspartoacylase (aminoacylase) 3	NM_027857	306	298	-	0.239
116	Asb-10	ankyrin repeat and SOCS box-containing 10	NM_080444	1338	1330	-	0.231
117	Wdr21	WD repeat domain 21	NM_030246	412	404	+	0.19
118	Pdlim4	PDZ and LIM domain 4	NM_019417	1371	1363	-	0.102
119	Acsm5	acyl-CoA synthetase medium-chain family member 5	NM_178758	1356	1348	+	0.0961
120	Apba3	amyloid beta (A4) precursor protein-binding, family A, member 3	NM_018758	844	836	+	0.0753

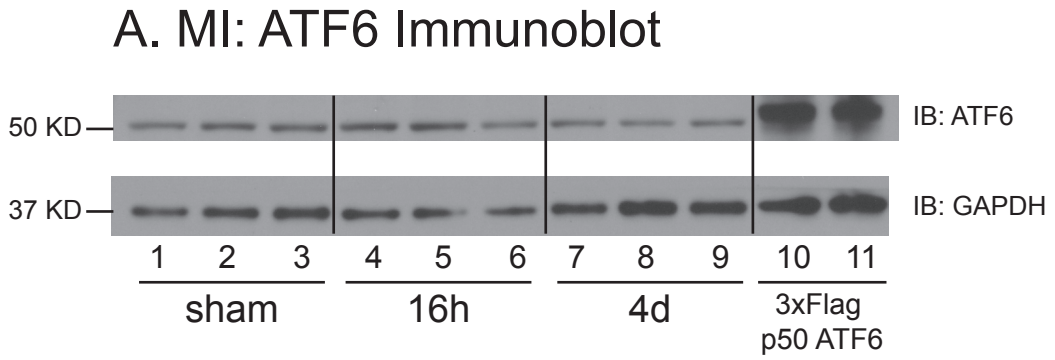

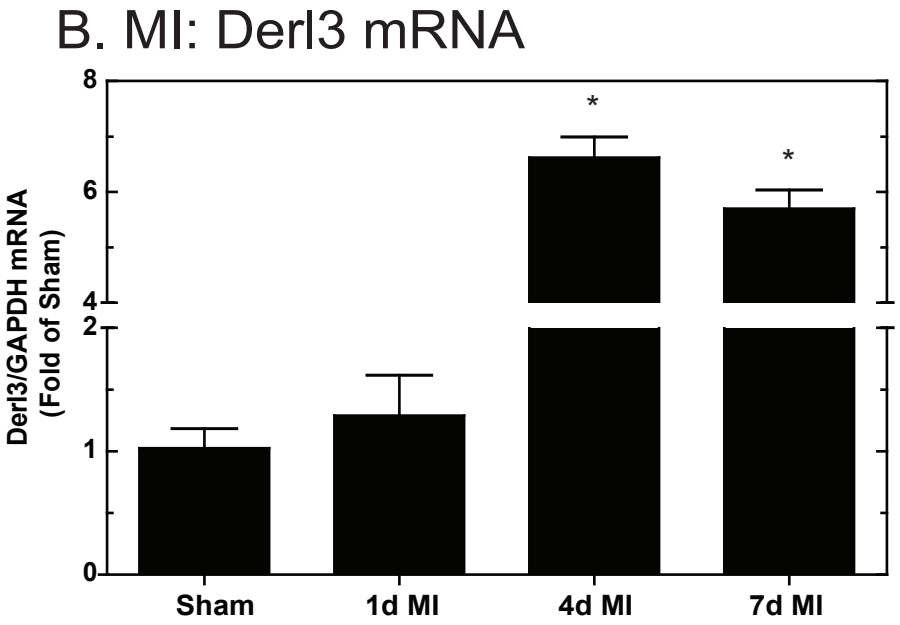

Online Figure I. Confirmation of 50KD ATF6 Protein and MI Induction of Derl3 mRNA
Panel A: NTG mice were subjected to sham infarct surgery or to permanent occlusion myocardial infarction for the indicated times. Animals were then sacrificed and hearts were used to prepare tissue extracts for western blot analysis, as previously described10 (lanes 1-9). To confirm the identity of the 50KD band, cell lysates from HeLa cells transfected with a 3xFlag-tagged ATF6 plasmid and subjected to the protease inhibitor ALLN (3mM) in order to preserve the labile, N-terminal form of ATF6, were loaded (lanes 10-11).
Panel B: NTG mice were subjected to sham infarct surgery or to permanent occlusion myocardial infarction for 1d, 4d, or 7d. Animals were then sacrificed and hearts were used to prepare tissue extracts for RT-qPCR, as previously described.10 The numbers of animals used for each trial were as follows: sham n = 4; MI n= 7 to 8. * = $p<0.05$ different from all other values determined by ANOVA.

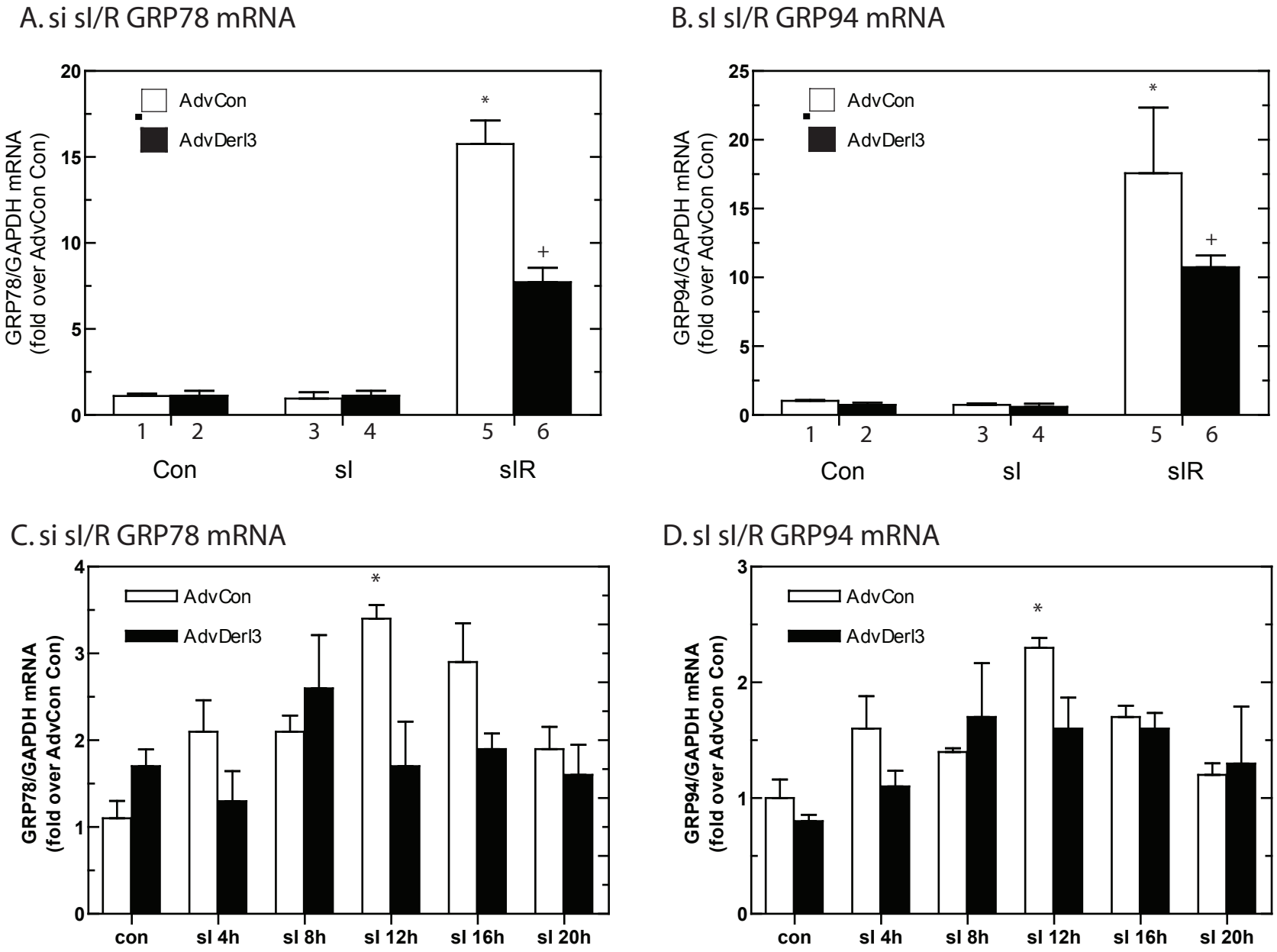

Online Figure II. Derl3 Overexpression Attenuates ER Stress mRNA Activation Following sI and sI/R:
NRVMCs were infected + AdVCon or AdV-Derl3 and 24h later, cultures were treated + sI for 20h followed by sI/R for 24h **(Panels A and B)**, or + sI for the indicated times **(Panels C and D)**. Cultures were then extracted and cell lysates were analyzed for the levels of the prototypical ERSR mRNAs, GRP78 and GRP94 (n = 3 cultures per treatment, sum of 2 separate experiments). Shown is the relative amount of each target mRNA/GAPDH, expressed as fold of AdVCon Con, + S.E for each treatment. Panels A-B: *, + = $p<0.05$ different from all other values by ANOVA, Panels C-D: * = $p<0.05$ from AdVCon Con by ANOVA.